ABSTRACT

KINETICS OF ELECTRON-ATTACHMENT REACTIONS
IN ANHYDROUS ETHYLENEDIAMINE

by Larry H. Feldman

The reaction of the solvated electron with water is of particular importance to radiation chemists (1). Preliminary studies by Dewald *et al.* (2) using solutions of cesium in ethylenediamine to measure the rate of this reaction by the stopped-flow method have been followed by a more extensive study of this system and extended to the other alkali metals.

The stopped-flow apparatus was modified to include a rapid-scanning monochromator and detection system capable of making from three to 150 spectral scans per second. The reaction system is thermostatted and uses Pyrex mixing cells. This arrangement permits study of rapid changes in the spectrum for suitable moderately fast reactions. The instrument is double-beam and direct reading in absorbance units. Data are stored on an FM tape recorder and played back to an oscilloscope. Tests of the instrument's performance are given.

These studies of the reaction of cesium with water in ethylenediamine verify the earlier rate constant

($k \sim 20\ M^{-1}sec^{-1}$), and in many cases show the presence of a slower second-order process ($k \sim 5\ M^{-1}sec^{-1}$). Similar results are found for the reactions of rubidium and potassium with water. The reaction of sodium with water in ethylenediamine is first-order in metal absorbance, but the order in water varies with the water concentration. Lithium-water reactions yield as many as three second-order rate constants, yet the lithium solutions used showed primarily an infrared band. The results are discussed in light of current models for metal-amine solutions and are correlated with the known absorption spectra (3).

Preliminary studies of the rate of reaction of metal-amine solutions with electron acceptors other than water have been made. Reactions with methanol and ethanol show rates similar to those with water. In addition, the presence of an absorbing intermediate was indicated, which will warrant more detailed examination. The rate constants for the reactions of cesium solutions with ethylenediammonium and ammonium ions were found to be 1.7×10^5 and a lower limit of $3 \times 10^6\ M^{-1}sec^{-1}$, respectively. The latter value is in agreement with the results of radiation chemistry (4), while the former has not been previously determined. Possible mechanisms for these electron-attachment reactions are discussed and suggestions for further work are made.

REFERENCES

1. M. Anbar, Advances in Chemistry Series, 50, "Solvated Electron," edited by R. F. Gould, American Chemical Society, Washington, D. C., 1965, p. 55.

2. R. R. Dewald, J. L. Dye, M. Eigen, and L. de Maeyer, J. Chem. Phys., 39, 2388 (1963).

3. R. R. Dewald and J. L. Dye, J. Phys. Chem., 68, 121 (1964).

4. J. Rabani, p. 242 in Ref. 1.

KINETICS OF ELECTRON-ATTACHMENT REACTIONS IN ANHYDROUS ETHYLENEDIAMINE

By

Larry H. Feldman

A THESIS

Submitted to
Michigan State University
in partial fulfillment of the requirements
for the degree of

DOCTOR OF PHILOSOPHY

Department of Chemistry

1966

To my Parents and Sharon

ACKNOWLEDGEMENTS

The author wishes to express his sincere appreciation to Professor James L. Dye for his guidance, encouragement, and keen insight throughout the course of this investigation and preparation of this thesis.

The advice of Dr. Robert R. Dewald during the initial phase of this work is gratefully acknowledged. Many thanks are due Messrs. Eklund, Grumblatt, Hansen, Seer, and Wreede for their technical assistance.

This research was supported by the United States Atomic Energy Commission and the Rapid Scan Monochromator was purchased in part through a grant from the Petroleum Research Fund of the American Chemical Society.

****

TABLE OF CONTENTS

TABLE OF CONTENTS - Continued

LIST OF TABLES

LIST OF FIGURES

LIST OF FIGURES - Continued

I. INTRODUCTION

Hart (1) has pointed out that solvated electrons, resulting from the interaction of ionizing radiation with water, have been present on this planet for four billion years. So reactive is this species, that its existence has been demonstrated only very recently (2-4). In 1864, Weyl observed that alkali metals dissolve in liquid ammonia (5), and in 1908, Kraus proposed on the basis of electrolytic experiments that the anionic species was, in fact, the ammoniated electron (6).

Metal-ammonia solutions have been studied in great detail in a number of laboratories. At the recent Weyl Colloquium, the physical properties of metal solutions were reviewed and models to explain these properties proposed (7). Since this time considerable work has been done and will be reviewed in some detail in Chapter II.

Alkali metals are soluble in several primary aliphatic amines, certain ethers, and other solvents. The existence of solvated electrons in many solvents other than water has been established by radiation chemists (8). An important aspect of radiation chemistry has been the measurement of the rates of reaction of e^-_{solv} with different chemical species. Most of the work to date has been with e^-_{aq} as the

reducing species. Over 300 different compounds have been investigated for their reactivity with e^-_{aq} (9). These bimolecular kinetic studies are necessarily limited to the range $k > 10^5\ M^{-1}sec^{-1}$ because of competing reactions with impurities and/or solvent. From the viewpoint of radiation chemists, the reaction

$$e^-_{aq} + H_2O \longrightarrow H + OH^-_{aq}$$

is the most important reaction in aqueous radiation chemistry. Were it not for the slowness of this reaction, $k = 16 \pm 1\ M^{-1}sec^{-1}$ (10), only the fastest reactions of the hydrated electron could be studied.

The reaction of solvated electrons with water has also been studied by Dewald and co-workers (11,12) who reacted solutions of cesium in ethylenediamine using the stopped-flow method, and followed the decay in electron absorbance as a function of time. A rate constant of $24.7 \pm 1.5\ M^{-1}sec^{-1}$ at room temperature was reported.

These studies pointed to possible use of such a system for the study of other electron-attachment reactions. In this research, studies using the cesium-water system were further pursued, but complications developed almost at once. A second, slower reaction was found to occur and the data showed an abnormal amount of scatter from run to run. The resolution of these difficulties has formed a major part of this investigation. Reaction of other alkali metal-water

systems in ethylenediamine, as well as a number of other electron-attachment reactions, have been examined.

In the course of this work, a number of experimental techniques were developed for the preparation of anhydrous solvents and metal-amine solutions. The stopped-flow apparatus has been modified and made more sophisticated by including a rapid-scanning monochromator and associated electronics.

II. HISTORICAL

A. Metal-Ammonia Chemistry

The blue color of dilute metal-ammonia solutions is a familiar phenomenon, and probably is what initially intrigued most investigators. In concentrated solutions, however, there is a metallic copper-like appearance and, in some cases, phase separation. If proper attention is paid to cleanliness and purity of materials, a stable solution can be obtained. Failure to observe such precautions can lead to false or incomplete results because of the decomposition reaction

$$M + NH_3 \longrightarrow MNH_2 + \tfrac{1}{2} H_2 \qquad (1)$$

Using EPR techniques, Kirschke and Jolly (13) have demonstrated that the reverse of this reaction can be made to occur to a slight extent.

The physical properties of dilute solutions of alkali metals in liquid ammonia have been studied extensively by a wide variety of methods. Some studies have also been made using solutions of alkaline earth metals. These investigations have been the subject of a number of reviews (7,14-17) and will only be considered briefly here.

The following methods have been used: electron paramagnetic resonance, static magnetic susceptibility, nuclear magnetic resonance, conductivity, electromotive force, transference number measurements, x-ray diffraction, photoelectric effects, the thermo-electric effect, optical absorption spectroscopy, vapor pressure studies, compressibility and viscosity, density and volume expansion, photolysis (18), and electron nuclear double resonance (ENDOR) (19).

Unfortunately, investigators in this field often propose a model which fits the results of a particular set of measurements, but which is inconsistent with those of another set. Any valid model proposed for these systems must explain:

1. The presence of a single asymmetric optical absorption band that peaks near 7000 cm^{-1}, has no observable fine structure, and obeys Beer's Law (20-22).

2. The volume expansion of metal-ammonia solutions, including the minimum found with sodium-ammonia and potassium-ammonia solutions (23-25).

3. Electrical properties: the fraction of current carried by the anionic species varies from 0.8 in dilute solutions to more than 0.99 for concentrated solutions in the neighborhood of 1 M (17, 26); concentrated solutions exhibit high electrical conductances characteristic of metals (27), while

more dilute solutions exhibit electrolytic conductance; a minimum in the equivalent conductance occurs at about 0.05 M (28).

4. The results of static field magnetic susceptibility measurements (29,30) as well as those of electron paramagnetic resonance (31), which indicate the need for diamagnetic species because of a rapid decrease in molar susceptibility with concentration.

5. Knight shifts and relaxation times of alkali-metal and nitrogen nuclei (32) and protons (33) in metal-ammonia solutions.

Several models have been proposed, none of which has been fitted to all of the data. These are reviewed below.

The earliest model, proposed by Kraus (6), assumed the presence of undissociated sodium atoms, sodium ions, and solvated electrons according to the equations

$$Na = Na^{+} + e^{-} \qquad (2)$$

$$e^{-} + x(NH_3) = (NH_3)_x e^{-} \qquad (3)$$

A number of observations led to the realization that the electrons in metal-ammonia solutions are trapped rather than free. Ogg (34) postulated that the solvated electron could be considered as trapped in a spherical cavity surrounded by ammonia molecules. He assumed that the electron is confined by an infinitely steep spherical potential well.

The wave function of the electron according to this model is that for a particle in a spherical box of radius R_o,

$$\psi = \frac{1}{2\pi R_o} \frac{\sin(\pi r/R_o)}{r} \qquad (4)$$

The zero point kinetic energy is $h^2/8mR_o^2$ while the polarization energy of the dielectric is $-\frac{e^2}{2R_o}(1 - \frac{1}{D_s})$, where D_s is the static dielectric constant of ammonia. The total energy is then given by

$$E = \frac{h^2}{8mR_o^2} - \frac{e^2}{2R_o}(1 - \frac{1}{D_s}) \qquad (5)$$

Minimizing E with respect to R_o, letting $1/D_s \sim 0$, gives

$$E = -\frac{me^4}{2h^2} = -0.38\text{eV} \qquad (6)$$

and

$$R_o = \frac{h^2}{2me^4} = 9.9\ \text{Å} \qquad (7)$$

This treatment leads to an underestimate of the enthalpy of solution and to an overestimate of the cavity radius. Lipscomb (35) refined these approximate calculations by incorporation of several additional contributions to the energy of the system: electrostriction, electronic polarization of the molecules on the cavity surface, and surface tension. Stairs (36) further improved these calculations by making a better estimate of the wave function using a graphical method of integration.

A natural extension of the primitive cavity model assumes that the surrounding solvent molecules do not provide

an infinite potential well for the electron. Thus the charge distribution of the extra electron can extend into the medium beyond the cavity boundaries (37). Application of polaron theory by Jortner (38) considers the interaction between the electron and the polarization field of the medium. This approach is an improvement upon a similar treatment given by Davydov (39) and Deigen (40), who also used polaron theory to theoretically treat metal-ammonia solutions.

In Jortner's treatment (38) the polarization is considered to be composed of two parts, the total polarization and the electronic polarization. The difference between these is the "permanent polarization" which creates the potential well. The electrostatic potential resulting from this polarization is assumed to be continuous up to R_o, the cavity radius, and constant within the cavity. A one parameter hydrogen-like wave function of the form

$$\psi_{1s} = \frac{\mu^3}{\pi} \exp(-\mu r) \qquad (8)$$

is used for the ground state and the energy of the ground state is calculated from the variation integral

$$W_{1s} = \int_v \psi_{1s} \left[- \frac{h^2 \nabla^2}{8\pi^2 m} + V(r) \right] \psi_{1s} \, dv \qquad (9)$$

by putting $\partial W_{1s} / \partial \mu = 0$. In this model the electronic polarization will lower the energy of this state by an additional amount. Agreement between this model and experiment is fairly good, considering the number of approximations

involved (17,38). An improvement in these calculations has been made by Jortner, Rice, and Wilson (37) using a self-consistent field approach. This treatment, however, does not enhance agreement with experiment. The experimental value of the enthalpy of solution is 1.7 ± 0.7 eV, and the value calculated by Jortner (38) is 1.60 eV, while the SCF value (37) is 0.92 eV.

A model that has seen considerable popularity is that of Becker, Linquist, and Alder (41) (BLA model), which is sometimes referred to as the cluster model. It is assumed that the metal atom is ionized and that the electron is trapped by the potential produced by the metal ion and the oriented ammonia molecules around the ion. In addition to this "monomer" species, a solvated metal ion, an electron arising from the dissociation of the monomer, and a dimer consisting of two monomers bound principally by exchange forces are postulated. The model involves consideration of the competition of two equilibria

$$M = M^{+} + e^{-} \qquad (10)$$

and

$$M_2 = M + M \qquad (11)$$

Presumably the electrons are solvated, but no explicit mention of their state is made (41). The BLA model has been used successfully to fit conductivity (26,41,42) as well as magnetic susceptibility data (41).

Gold, Jolly, and Pitzer (43) have pointed out that the BLA model is not consistent with optical, volumetric, and NMR data. These authors propose instead that the monomer is a simple ion-pair consisting of an ammoniated metal ion and an ammoniated electron. The dimer species, M_2, is pictured as a quadrupolar ionic assembly of two solvated electrons and two solvated metal ions in which there is little distortion of the solvated species. On the basis of Jortner's calculations (38), they assume that the wave functions for the two e^-_{am} in M_2 will overlap significantly, and further that the singlet will be lower in energy than the triplet by more than kT. In this way, at least qualitatively, optical, volumetric, and Knight shift data are explained (43). It should be pointed out that O'Reilly (44) has recently used the BLA model to successfully fit Knight shift and relaxation time data (32). He was also able to calculate spin densities at the nitrogens of the cavity species which are in good agreement with experiment (44).

When calculating equilibrium constants from experimental data, either the BLA monomer or an ion pair, $M^+ \cdot e^-$, can be used for the M species in Equation 10. However, the constants calculated from conductivity data differ from those obtained using magnetic susceptibility data (45). These difficulties can be overcome by introducing another species, $(M')^-$ and a third equilibrium,

$$(M')^- = M + e^- \qquad (12)$$

Such a scheme has been proposed by Arnold and Patterson (46,47) and by Golden, Guttman, and Tuttle (48). The M' center is diamagnetic and negatively charged.

Arnold and Patterson (47) made no assumption about the exact nature of the various centers but confined their discussion to the calculation of the equilibrium constants for the various processes (Equations 10-12). The constant for Equation 10 was determined from conductivity data at low concentration and the other constants were computed from transference number and susceptibility data. Agreement with experiment is good, even at high concentrations, but three adjustable parameters are required.

The model of Golden et al. (48) introduces the metal anion, M^-, for the M' species. Equations 10-12 would then be rewritten as

$$M^+ \cdot S^- = M^+ + S^- \qquad (10')$$

$$M^+ \cdot M^- = M^+ + M^- \qquad (11')$$

and

$$M^- + 2S = M^+ + 2S^- \qquad (12')$$

where S is solvent and S^- is equivalent to e^-_{solv}. Using this scheme and only a single adjustable parameter, they obtain good agreement with vapor pressure, conductivity, Knight shift, and optical absorption data. The last comparison, however, according to Jolly (49), may be in error. By a thermodynamic argument, Golden et al. (48) show that

the M^- species is not equivalent to the ion triple, $S^-\cdot M^+\cdot S^-$. This argument is only valid for non-polarizable hard sphere ions and neglects consideration of wave function overlap in the ion triple as a mechanism to lower its energy. The data they used cannot, in fact, distinguish among the various descriptions of the species. The advantage of the treatment of Golden et al. over that of Arnold and Patterson is the reduction of the number of adjustable parameters from three to one.

B. Metal-Amine Chemistry

Alkali metals dissolve in many primary aliphatic amines, several ethers, and in a few other oxygen containing solvents (11). In all cases, the blue color characteristic of metal-ammonia solutions appears. Work with metal-amine solutions has been less extensive than with metal-ammonia solutions. A possible reason was the lack of stability of the former as compared to that of the latter. Analogous to Equation 1, these solutions can decompose with the evolution of hydrogen

$$M + RNH_2 \longrightarrow M(RNH) + \tfrac{1}{2} H_2 \qquad (13)$$

Recent results in a number of laboratories have indicated that this reaction is not much faster than the corresponding reaction in liquid ammonia (after adjustment for temperature differences), and with proper care its effect can be minimized. This could lead to an increase in the number of workers in the field.

A summary of earlier studies of optical absorption spectra (50) and conductivities (51) is given by Dewald and Dye. In these papers, and in Reference 11, aside from presenting extensive experimental results for metal solutions in ethylenediamine (EDA), the authors pointed out the need for a model for metal-amine solutions which did not simply modify existing models for metal-ammonia solutions (52), but added other species.

Dewald and Dye (50) observed one to three very intense absorption bands depending upon the alkali metal used. One of these peaks appeared in the visible region at 650 mμ (V band), one in the near-infrared region at 800 to 1100 mμ (R band), and the third in the infrared at 1300 mμ (IR band). The V band is present in lithium, sodium, potassium, and rubidium solutions and its shape and position are independent of metal, but the intensity relative to the IR absorption depends strongly upon the metal. Solutions of potassium in EDA show the R band at 845 mμ, rubidium at 890 mμ, and cesium at 1030 mμ. All solutions show IR absorption, but in sodium solutions this absorption is negligible compared with that of the V band. The various bands are only slowly interconverted.

The conductances of cesium, rubidium, potassium, and lithium in EDA show the same general concentration dependence, while sodium solutions exhibit a marked difference in behavior (51). Dye and Dewald (52) postulate that the IR species in these EDA solutions are "ammonia-like" in nature

containing species consistent with the model of Gold, Jolly, and Pitzer (43), and that the metal-dependent R band is due to covalent dimers similar to those found in alkali metal vapors. The V band was attributed to an electron trapped by a solvated M_2^+ ion in the same way that the electron is presumed trapped in a BLA monomer unit (41). The possibility that the V species was in fact a BLA monomer was ruled out on the basis of the slow conversion of this species (52). These assignments were supported by thermodynamic estimates and the ability of the model to account for the diverse results reported by others (52).

The discovery of nuclear hyperfine splitting by the metal nucleus in metal-amine solutions (53,54) has introduced a powerful and sensitive method for examining the paramagnetic species in these solutions. Bar-Eli and Tuttle (55) studied the EPR spectra of solutions of potassium and lithium in ethylamine, potassium in methylamine, and potassium and lithium in mixtures of these amines. They have also examined rubidium and cesium in ethylamine (56). The hyperfine splitting obtained in these solutions is strongly dependent upon temperature and solvent composition. A striking example of the latter is seen in the work of Dalton and co-workers (57) on the EPR spectra of potassium in ethylamine-ammonia mixtures. In samples containing 0.6 to 23.4 mole-percent ammonia the hyperfine splitting changed from 11.52 to 2.64 gauss at 25° C, and corresponding changes were observed at other temperatures. Bar-Eli and Tuttle (55) interpreted

these phenomena in terms of a modified BLA model, while Dalton et al. (57) quantitatively described the temperature dependence with a model involving equilibrium between atoms and monomers, and introduced an additional monomeric species (one in which an ammonia molecule has replaced ethylamine) to explain the dependence upon ammonia concentration. O'Reilly and Tsang (58) have sought to explain the temperature dependence of these solutions in terms of the combined action of solvent-molecule polarizability and an expansion of the monomer with temperature.

Ottolenghi and co-workers (59) have assigned the V band to the monomer and the R band to a dimer for metal solutions in ethylamine. This assignment is based upon the observed constancy of the ratio of $D^2_{650\ m\mu}$ to $D_{850\ m\mu}$ for both potassium and rubidium in ethylamine, where D is absorbance. They also observed that the decay of the EPR absorption closely followed that of the V band for solutions of potassium in ethylamine. Similar results for the ratio $D^2_{600\ m\mu}$ to $D_{1000\ m\mu}$ have been reported by Ottolenghi and Linschitz (18) in both the original and in photo-regenerated potassium and rubidium solutions in ethylamine.

It has been shown conclusively by Dye, Dalton, and Hansen (60) and by Dalton et al. (57) that the species responsible for the V band and that giving rise to the hyperfine splitting (monomer) are not the same. Their arguments are based upon determination of spin concentrations, opposite

changes in V band absorbance and number of spins as a function of temperature, dependence of spin concentration of the hyperfine species and the absorbance of the V band upon ammonia concentration, and the kinetics of decomposition. The latter was found to yield a D_{650} to D_{850} ratio of nearly unity for potassium in ethylamine (57) and for extensive kinetic studies (61) of alkali metals in EDA. Thus the nature of the V species is still largely a matter of conjecture, but it is not the same as the species observed by EPR.

Ottolenghi and co-workers (62) demonstrated a large shift of the maximum of the R band towards the blue with temperature for solutions of potassium, rubidium, and cesium in ethylamine. Such a shift is not consistent with the previous assignment (52) to the $^1\Sigma_u^+ \leftarrow {}^1\Sigma_g^+$ transition of an alkali metal dimer. Recent measurements on the spectra of gaseous Rb_2 and Cs_2 show that the absorption should probably be assigned to the $^1\pi_u \leftarrow {}^1\Sigma_g^+$ transition shifted to lower energies by the interaction with solvent (63). Alternatively, the intermediate absorption could be due to another type of species.

Anbar and Hart (64) have studied the properties of an electron-pulse-generated species in ethylenediamine. They observed only one band with a maximum at 920 mμ and a two μsec. half-life, and attributed this to the solvated electron. This does not agree with the earlier assignment based on

spectra and conductivity (50-52). Recently, this system has been re-examined (102) and the earlier peak was found to be an artifact of the measuring technique. The absorbance of the transient produced by pulse radiolysis rises continuously from 700 mμ to the limit of the method (~1100 mμ). This strengthens the assignment of the IR band to the solvated electron.

C. Radiation Chemistry

Historically, the evolution of gas from aqueous solutions containing radium salts was one of the earliest radiation-induced chemical reactions to be observed and studied. Both oxidation and reduction of dissolved substances were observed, and as far back as 1914, Debierne (65) suggested that free radicals from the water might be responsible for the chemical action of radiation.

In 1959, Barr and Allen (66) showed that the hydrogen "atom" ($H^{'}$) formed in the radiolysis of neutral aqueous solutions containing hydrogen, oxygen, and hydrogen peroxide by oxidation of hydrogen

$$OH + H_2 \rightarrow H^{'} + H_2O \qquad (14)$$

reacts with oxygen much faster than with hydrogen peroxide, while for solutions containing only oxygen and hydrogen peroxide, the rates of reaction with hydrogen "atoms" produced by water radiolysis are comparable. They concluded

that the two types of hydrogen atoms were different, and that one was atomic hydrogen and the other an acidic or basic form of the hydrogen atom. The pH dependence in the radiolysis of aqueous systems provided further evidence for this hypothesis (67,68). The species present in acid solution, H_a, can be formed from H_b by

$$H_b + H_3O^+ \rightarrow H_a \qquad (15)$$

This reaction has a pK value of about 3 (69). H_2^+ was eliminated as a kinetically important acid form by Czapski, Jortner, and Stein (70) who produced H atoms by electrodeless discharge and showed that the reaction

$$H + H_2O_2 \rightarrow OH + H_2O \qquad (16)$$

was unaffected by pH from 1-13. A number of experiments (71) showed H' to be atomic hydrogen, and Czapski and Schwartz (72) utilized the kinetic salt effect to demonstrate that the reducing radical produced in the cobalt-60 radiolysis of water has a unit negative charge and may be considered a solvated electron. Recent work using pulse radiolysis confirming these results has been reviewed by Matheson (73).

Hart and Boag (2,3), using a pulsed beam of electrons to irradiate pure deaerated water, observed a transient absorption band peaking at 7200 Å. Since the spectrum was suppressed by known electron scavengers, such as H_3O^+, O_2, and N_2O, and resembled the absorption bands of the solvated

electron in liquid ammonia and methylamine, it was identified as that of the hydrated electron. The results of Keene (4) confirmed these observations. The probable existence and properties of the hydrated electron had been predicted earlier by Platzman (74). Since its discovery in 1962, a number of the properties of the hydrated electron have been determined and are summarized in Table I.

The initial effect of ionizing radiation on pure liquid water is to strip off electrons from the water molecules in the path of the beam. It is believed that the products of radiolysis (e^-_{aq}, H, OH, H_3O^+, OH^-, H_2O_2, and H_2) are formed within 10^{-8} sec. What probably happens before this time has elapsed is reviewed by Spinks and Woods (71) and will not be discussed here. A number of investigators include activated water molecules, H_2O^*, in the list of initial radiation products (75). The existence of holes or positive polarons, H_2O^+, has been discussed by Moorthy and Weiss (76) in the irradiation of frozen aqueous solutions at 77^o K, but their presence in liquids has not been demonstrated.

Reactions of the hydrated electron are numerous, and a recent review by Anbar (9) discusses a number of them in detail. The reaction

$$e^-_{aq} + H_2O \rightarrow H + OH^-_{aq} \qquad (17)$$

is of particular importance to the radiation chemist. A summary of rate constants for the reactions that occur

Table I. Properties of the Hydrated Electron*

λ_{max}	7200 Å (1.72 e.V.)
Molar extinction coefficient at 5780Å	10,600 (± 10%) $M^{-1}cm^{-1}$
at 7200 Å (max.)	15,800 $M^{-1}cm^{-1}$
f = oscillator strength	0.65
Charge	-1
pK_a ($e^-_{aq} + H_2O = H + OH^-_{aq}$)	9.7
Hydration energy (calc.)	$\geq$ 1.72 e.V.
E^o ($e^-_{aq} + H_3O^+_{aq} \rightarrow \frac{1}{2} H_2 + H_2O$)	$\leq$ 2.67 volts
$\tau_{\frac{1}{2}}$ (pure water at pH 7.0)	780 μsec (Ref. 10)
Diffusion constant	4.5×10^{-5} (± 15%) cm^2/sec
Mean radius of charge distribution (calc.)	2.5 - 3.0 Å
$G_{e^-_{aq}}$ (in neutral water)	2.6

*From Matheson (73).

between many of the primary radiolysis species, taken from Matheson (73), is presented in Table II. Since Reaction 17 is slow, it does not interfere appreciably with these reactions.

The reverse of Equation 17,

$$H + OH^- \longrightarrow e^-_{aq} + H_2O \qquad (18)$$

has been studied in detail (77,78) and a rate constant of 2.2×10^7 $M^{-1}sec^{-1}$ obtained (78). Combining this with the value of 16 $M^{-1}sec^{-1}$ (10), obtained for Reaction 17, gives a pK_a of 9.6 for the equilibrium

$$e^-_{aq} + H_2O = H + OH^-_{aq} \qquad (19)$$

It has been proposed that e^-_{aq} reacts with Brönsted acids following the Brönsted general acid catalysis law (78). Anbar (9) has reviewed evidence contrary to this hypothesis and suggested instead that the electron is incorporated into the acid to form an AH^- radical, which may subsequently undergo decomposition.

In addition to Reaction 17, e^-_{aq} may disappear by the bimolecular process

$$e^-_{aq} + e^-_{aq} \longrightarrow H_2 + 2OH^-_{aq} \qquad (20)$$

It has been shown conclusively (77,79) that this reaction produces molecular hydrogen, and that the hydrogen produced does not originate from the recombination of two H atoms or

Table II. Rate Constants in Pulse Radiolized Water*

Reaction	pH	Rate Constant ($M^{-1}sec^{-1}$)
1. $e^-_{aq} + H_2O \rightarrow H + OH^-_{aq}$	8.4	16 ± 1
2. $e^-_{aq} + H_3O^+_{aq} \rightarrow H + H_2O$	2.1-4.3	$(2.07 \pm 0.08) \times 10^{10}$
3. $e^-_{aq} + H_2O_2 \rightarrow OH + OH^-_{aq}$	7	$(1.23 \pm 0.14) \times 10^{10}$
4. $e^-_{aq} + e^-_{aq} \rightarrow H_2 + 2OH^-_{aq}$	10.9	$(0.9 \pm 0.15) \times 10^{10}$
5. $e^-_{aq} + H \rightarrow H_2 + OH^-_{aq}$	10.5	$(2.5 \pm 0.6) \times 10^{10}$
6. $e^-_{aq} + OH \rightarrow OH^-_{aq}$	10.5	$(3.0 \pm 0.7) \times 10^{10}$
7. $e^-_{aq} + O^-_{aq} \xrightarrow{H_2O} 2OH^-_{aq}$	13	$(2.2 \pm 0.6) \times 10^{10}$
8. $H + OH^-_{aq} \rightarrow e^-_{aq} + H_2O$	11.6	$(1.8 \pm 0.6) \times 10^{7}$
9. $H + H \rightarrow H_2$	2.1	2×10^{10}
10. $H + OH \rightarrow H_2O$	3	$(0.7 - 3.2) \times 10^{10}$
11. $H + H_2O_2 \rightarrow OH + H_2O$	2.1	$(9.0 \pm 1) \times 10^{7}$
12. $OH + OH \rightarrow H_2O_2$	7	$(1.26 \pm 0.16) \times 10^{10}$
13. $OH + H_2 \rightarrow H + H_2O$	7	4.5×10^{7}
14. $O^-_{aq} + H_2 \rightarrow H + OH^-_{aq}$	13.3	$(8 \pm 4) \times 10^{7}$
15. $OH + H_2O_2 \rightarrow H_2O + HO_2$	7	4.5×10^{7}
16. $H_3O^+_{aq} + OH^-_{aq} \rightarrow 2H_2O$	7	1.43×10^{11}

*From Matheson (73)

from e^-_{aq} and H in a cage. The exact mechanism of this reaction is not clear. Anbar (9) has speculated that it might proceed through an intermediate hydride ion, H^-, since hydride ion formation is thermodynamically feasible and H^- reacts with water at a diffusion-controlled rate.

Optical absorption spectra of the solvated electron have been reported for a number of liquids other than water. Sauer, Arai, and Dorfman (80) discuss the absorption spectra and yields of the solvated electron in the aliphatic alcohols by pulse radiolysis and the γ-radiolysis of ethanol is considered by Myron and Freeman (81). The results of Anbar and Hart (64) in ethylenediamine have been discussed previously (Sect. II-B). A reversible increase in the conductivity of liquid ammonia during γ-ray irradiation has been reported by Ahrens, Suryanarayana, and Willard (82) and an optical spectrum attributed to the solvated electron in ammonia was recently reported by Compton and co-workers (83). Other solvents, along with some theoretical correlations, are reviewed by Dorfman (8).

D. The Stopped-Flow Method

The stopped-flow method of Chance (84), as modified by Gibson (85), has been used by a number of investigators (86-88) to study moderately fast reactions with half-times from two milliseconds up to 100 seconds, and requires relatively small amounts of reagents. Precision is usually good

($\sim$5%), and the method only requires a rapid measurement of concentration changes.

When this technique is applied to systems exhibiting a color change during the course of reaction, several difficulties arise. It is generally not possible to study intermediates, or simultaneous reactions of species whose spectral bands are close together. For the most part, studies involving changes in absorbance as a function of time using this method have been carried out at one, or at most two, wavelengths at a time. On the other hand, the continuous flow method (87) requires a precisely known flow velocity and rather large amounts of reactant solutions.

The advantages to be gained from the ability to scan a large spectral region in a short period of time, have led to the development of several rapid-scanning monochromators (89,90). Incorporation of one of these (89b) into a stopped-flow system is discussed in Sect. III-G.

III. EXPERIMENTAL

A. General Laboratory Techniques

1. Glassware cleaning. The items were first rinsed briefly with a hydrofluoric acid-detergent cleaning solution (5% hydrofluoric acid, 33% concentrated reagent grade nitric acid, 2% acid soluble detergent, and 60% distilled water, by volume), then ten times or more with distilled water. Next, they were filled with fresh aqua regia and heated to boiling, followed by ten more rinses with distilled water, then by several rinses and/or soakings in double-distilled conductance water. After each use and a preliminary cleaning, they were heated in an annealing oven at 550° C before being cleaned as described above.

2. Vacuum technique. High vacuum techniques were used wherever possible with well-trapped mercury vapor diffusion pumps giving pressures between 10^{-5} and 10^{-6} torr, as read on a calibrated ionization gauge. Dow Corning high vacuum silicone grease was used on all stopcocks which came into contact with liquid; Apiezon N grease was used elsewhere. Apiezon T grease was used on movable tapers and ball joints, and Apiezon W wax was used on all fixed joints.

B. Metal Purification

Alkali metals of the highest purity commercially available were obtained from the following sources: sodium, J. T. Baker; potassium, Mallinckrodt; rubidium, Fairmount Chemical Company; cesium, a gift from the Dow Chemical Company; and lithium, Lithium Corp. of America.

To obtain small lithium samples free from oxide and nitride surfaces, the following procedure was used. A Caemco Model 39 dry-box was evacuated and filled with high purity helium (99.7%) which had been passed through an activated silica gel column at liquid nitrogen temperature. The glassware shown in Figure 1, a knife, a forceps, and a piece of lithium that had been washed with benzene were put into the dry-box airlock. After evacuation of the airlock and refilling with helium, these items were taken into the main box. The stopcock plug had been greased with Apiezon N grease and was kept apart from the stopcock barrel. A small piece of lithium, cut from the center of the larger piece, was placed in the stopcock against the break-seal as shown. Next a magnet sealed in glass was slipped into the stopcock, and finally the plug was inserted and turned to spread the grease. In most cases, the lithium would remain bright and shiny in the dry-box, but the use of phosphorous pentoxide as a desiccant seemed to help somewhat. The stopcock was then removed from the dry-box, pumped down to better than 10^{-5} torr, and sealed off where the glass had been thickened.

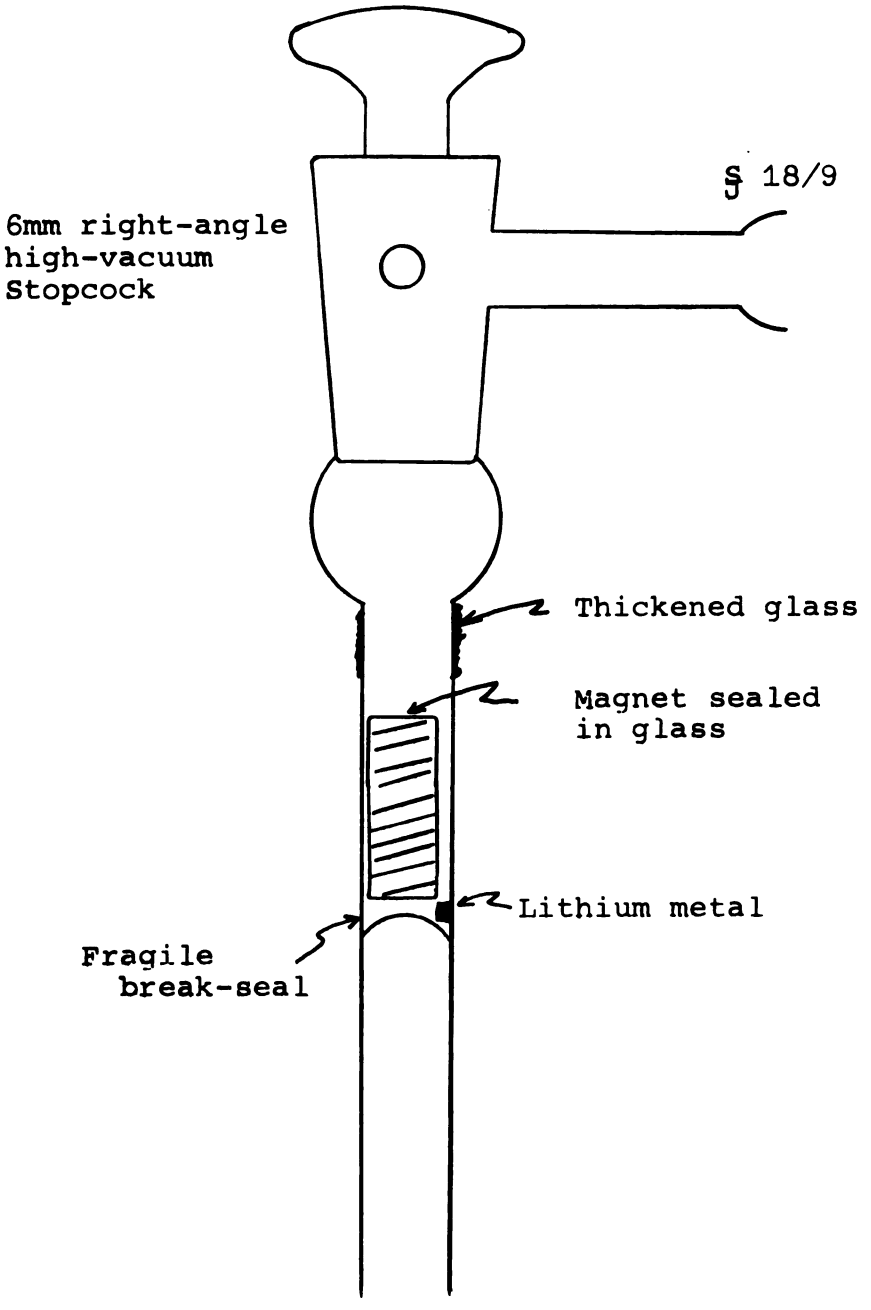

Figure 1. Lithium break-seal apparatus.

The other metals were cleaned, cut, and then degassed under high vacuum. Repeated vacuum distillations were used to obtain small metal samples in sealed ampoules which were used to make up metal solutions. Details of the techniques required are given by Dewald (11) and by Vos (91).

C. Solvent Preparation

Ethylenediamine (Matheson, Coleman, and Bell 98-100%) was purified in either of two ways. The first method (11,50) involved distillation at atmospheric pressure in a stream of nitrogen, followed by reaction with alkali metals, and repeated vacuum distillations. In the second method (for which we are indebted to Professor Paul Sears of the University of Kentucky), EDA was purified in a large separatory funnel by slowly freezing it and then melting and discarding the core (see Figure 2). Pre-purified nitrogen (Matheson) was used as a covering gas throughout this procedure. The process was repeated at least four times and resulted in a pure product, specific conductance = 10^{-7} $ohm^{-1}cm^{-1}$, without the difficulties involved in distillation.

Following freeze-purification, the EDA was put over sodium pieces in a flask (Figure 3 - flask no. 1) which had been evacuated with a mechanical pump through a trap at 77° K. When the bubbling had quieted down, small pieces of lithium metal were introduced by turning the sidearm, and a deep blue solution formed almost at once. The EDA was

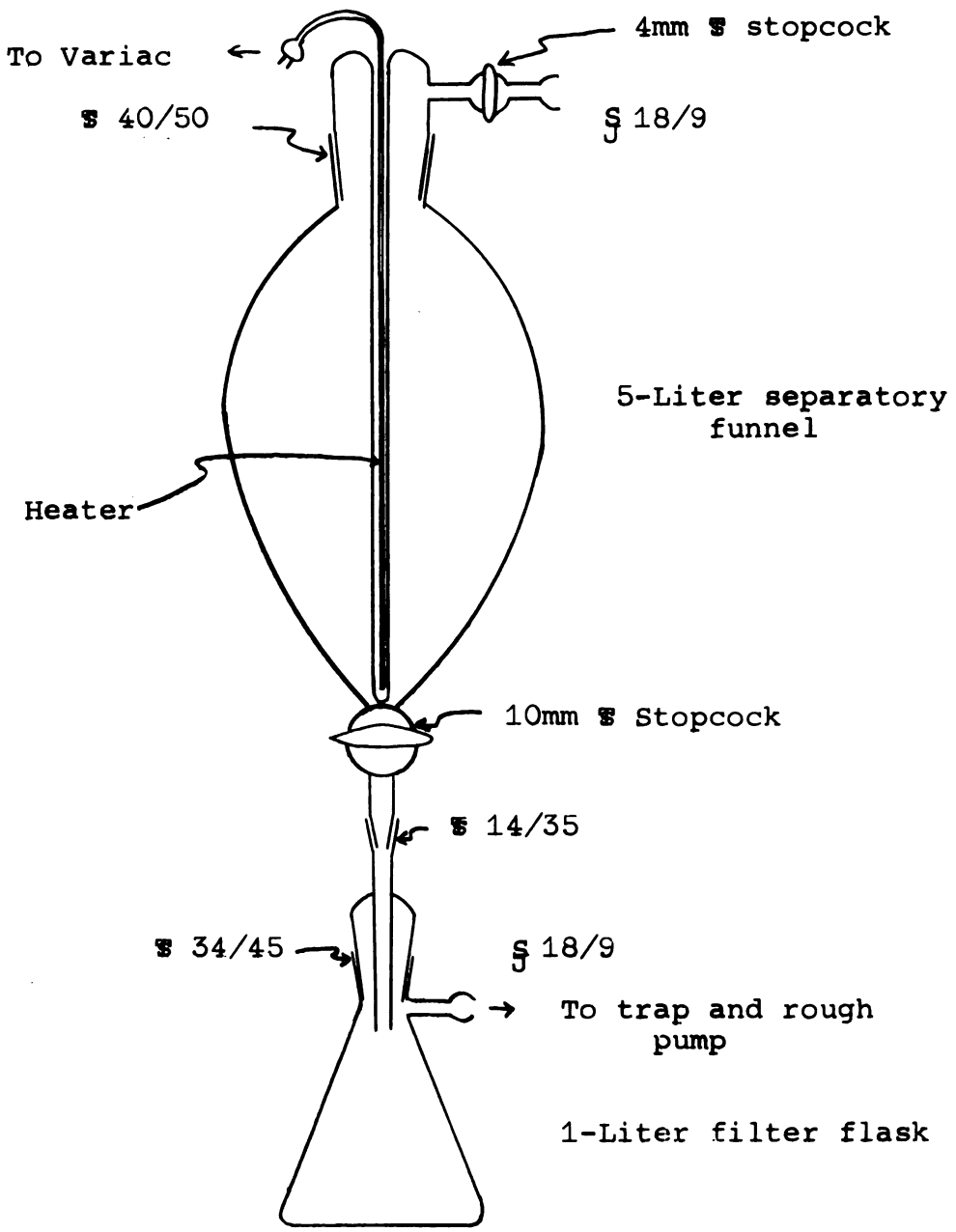

Figure 2. Freeze purification setup.

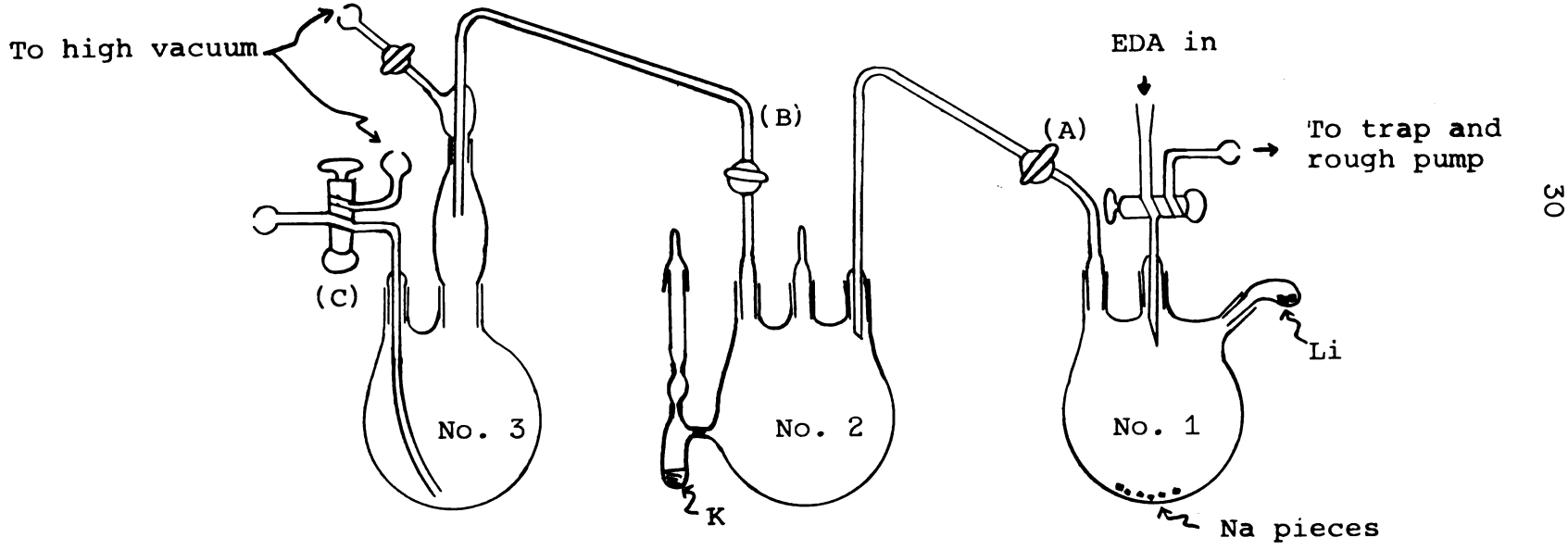

Figure 3. Ethylenediamine purification train.

then cooled using an ice-water mixture and degassed with a rough pump during freezing. Next it was thawed, allowed to stand for about a day, and frozen again. After thawing, the solution was pumped on with high vacuum and, from this point on, only high vacuum was used.

The solvent was then vacuum-distilled onto a potassium mirror which had been vacuum-distilled from the sidearm on flask no. 2. It took about a day to distill all of the EDA, and any hydrogen produced was pumped off from time to time. At this point, stopcock A was closed and freeze-purified EDA was again introduced into flask no. 1, and treated as described above. The EDA in flask no. 2, which had remained for about two days with potassium in solution, was next vacuum-distilled into flask no. 3. Then the EDA in flask no. 1 was distilled into flask no. 2, keeping stopcock B closed except when pumping off the hydrogen. After the distillation into flask no. 2 had been completed, stopcocks A and B were closed and the EDA in flask no. 3 was frozen, degassed, and covered with specially purified nitrogen (Sect. III-D). The EDA in flask no. 3 was drawn off as needed through stopcock C, and the EDA in flask no. 2 was vacuum-distilled to flask no. 3 when necessary. Since the metals were used up and the stopcocks gradually became "frozen," it was necessary to clean and reassemble the entire purification train for each double batch of solvent prepared.

D. Nitrogen Purification

Nitrogen (Matheson, pre-purified) was used as a covering gas for all liquids. It was further purified by passing it over copper turnings in a tube furnace, through an Ascarite column, a dry-ice trap, and finally a silica gel column at 77^{o} K in which some condensation occurred. This nitrogen was then stored in two-liter bulbs on the vacuum line.

E. Solution Make-up

Water solutions in ethylenediamine were made from freshly distilled conductance water that was degassed by repeated freezing and pumping, and then vacuum-distilled. Next it was either vacuum-distilled directly into a solution make-up flask or was used to prepare fragile glass ampoules, which could be used to make up water solutions of lower concentration. With proper care, solutions whose concentrations were known to one part per thousand could be made up. Complete details of these procedures are given in Reference 11.

Absolute methanol was distlled from a magnesium-magnesium sulfate mixture and then degassed and vacuum distilled. Spectral grade absolute ethanol was distilled after reaction with sodium metal, then degassed and vacuum-distilled. A solution of ethylenediammonium chloride ($EDAH^{+}Cl^{-}$) was prepared by introducing a known amount of hydrogen chloride gas (Matheson) into a solution make-up

flask. An ammonium bromide solution was made using the reagent grade salt. A cesium hydroxide solution was prepared using a cesium mirror onto which water treated as above was distilled. The concentration of cesium hydroxide is uncertain because of the separation of a small amount of a liquid-phase when EDA was added. These solutions were made up as soon before a given run as possible, but could be kept for as long as two months, if the flasks were sufficiently leak-tight.

Metal solutions were made up immediately prior to each run. The apparatus used is shown in Figure 4, which is after Dewald (11). After attaching this apparatus to high vacuum, a sealed capillary containing the required amount of metal was broken open and dropped into the sidearm on the metal make-up vessel, which was then pumped down to better than 10^{-5} torr. The metal was melted down into B, and A was pulled off under vacuum. The metal was degassed and the flask flamed until the pressure stabilized at better than 10^{-5} torr. Next, the metal was vacuum-distilled and B was pulled off under vacuum. EDA was introduced, the solution was stirred with the magnet sealed in glass, and any hydrogen produced was pumped off. Nitrogen was then put over the solution, about ten ml. were run into waste, and then about 30 ml. were run into the decomposition vessel for analysis. The metal-ethylenediamine solutions prepared in this manner were stable from eight to 24 hours without

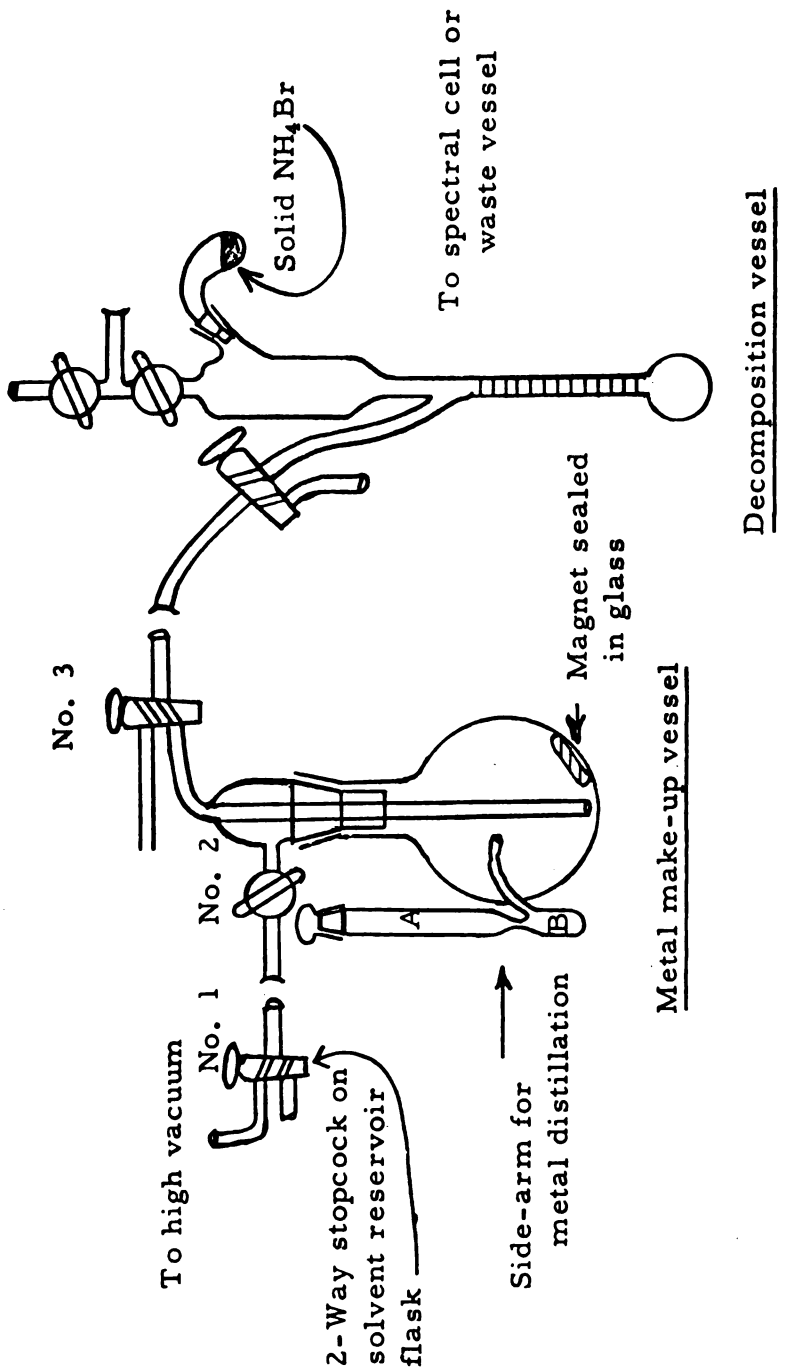

Figure 4. Metal solution make-up assembly [from Dewald (11)].

visible evidence of decomposition at room temperature. Metal concentration was determined by measuring the amount of hydrogen collected from a solution decomposed with ammonium bromide, since

$$NH_4Br + M(\text{in EDA}) \rightarrow \tfrac{1}{2} H_2 + MBr + NH_3$$

Lithium solutions could not be prepared as above, so a different procedure was followed. After seal-off of a lithium sample (Sect. III-B), the ampoule was carefully sealed to the metal make-up flask in place of the melt-down sidearm. After evacuation, the flask was filled with EDA and nitrogen covering gas put in as well. The break-seal was shattered only after the flask had been connected to the flow apparatus. Lithium solutions prepared in this fashion were not reproducibly stable, but did last as long as necessary for a run (four hours) in two of the three lithium runs.

F. Fixed Wavelength Stopped-Flow Apparatus

Only a brief description of this apparatus, shown schematically in Figure 5, will be given here, since construction details of a similar apparatus are given by Dewald (11) and elsewhere (92). The entire system, including syringes, could be pumped down to better than 10^{-4} torr. Only one concentration of the metal solution was used in a given run, while up to five concentrations of the more

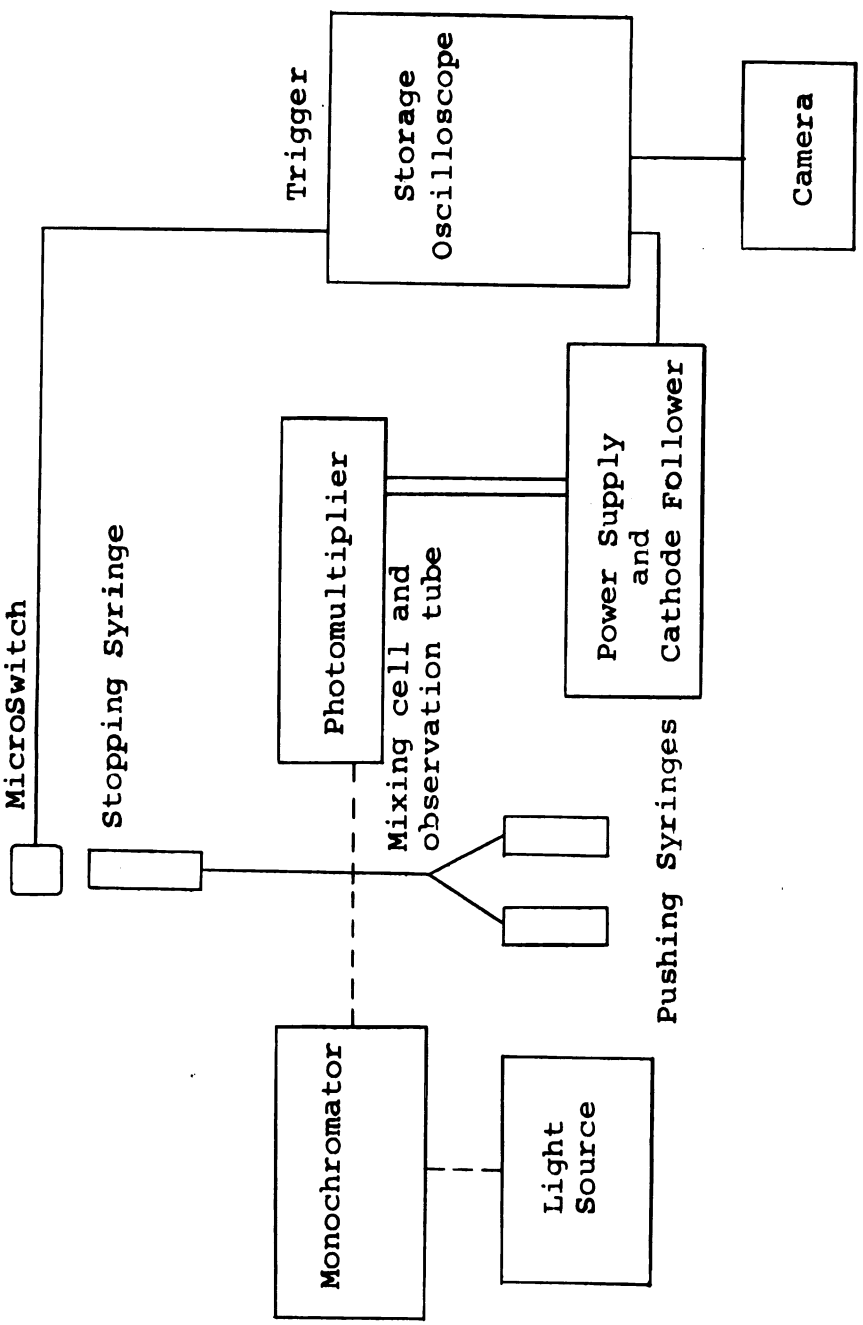

Figure 5. Block diagram of fixed wavelength stopped-flow apparatus.

stable solutions could be prepared in separate vessels and attached to the system. Dilutions with pure solvent were made with a thermostatted buret, and the solutions thoroughly mixed in a thermostatted vessel using a magnet sealed in glass. The syringes were also thermostatted using plastic jackets sealed with O-rings. The thermostatting fluid was circulated by a Lab-Line Hi-Lo Tempmobile.

The solutions were delivered via heavy-walled capillary tubing to their respective syringes. Pyrex ball joints were sealed to the syringes using uranium glass as an intermediate. Three-way high-pressure, vacuum-ground stopcocks, originally made in Germany but also available from H. S. Martin Co., were then turned to the mixing chamber and a lever depressed which pushed the syringes. A four-jet Plexiglas mixing chamber, which had four inlet holes of 0.5 mm bore each arranged almost tangentially about a 1.0 mm central hole, was used. This cell is capable of a mixing efficiency of better than 98% in two milliseconds, as measured by an acid-base reaction. The mixing cell was mounted upright to eliminate bubbles. It was gradually attacked by the solutions, and had to be changed every few runs.

To eliminate this difficulty, a four-jet Pyrex mixing chamber of 1.0 mm i.d. was constructed from precision-bore heavy-walled capillary which had been ground and polished by Precision Glass Products Co., Oreland, Pa. This cell was constructed by the University Glass Shop as follows: First

a steel template was machined so that four heavy-walled capillary sidearms of 0.5 mm i.d., when sealed to the central tube would have their bores arranged almost tangentially around the central hole and make an angle of about 105° with the capillary. The sidearms, closed at the end, were sealed to the central tube one at a time, taking care that the template remained hot during the process. A tungsten rod ~ 0.5 mm in diameter was twisted almost into the central tube using the radiant heat from the rod to soften the glass ahead of it. The hole was completed from above and the procedure repeated. Then the central hole was closed by melting a fitted glass rod which rested on a tungsten rod that had been inserted through one of the sidearms, and finally this area above the mixing chamber was flattened using a carbon rod. These cells were found to perform as well as the plastic cells.

Since Pyrex is not suited for work below about 320 mμ, two cells were constructed from fused quartz by W. A. Eberhart, Windsor, Ontario. The basic design is similar to that described above, but the holes into the central tube were precision drilled. The cost of these cells is at least ten times that of the Pyrex cells.

When flow was stopped by the filling of a third syringe against a metal plate, a micro-switch triggered the time base of a Tektronix Model 564 Storage Oscilloscope. The vertical deflection on the scope produced by the output of the photomultiplier (RCA 7102 or 6199, depending upon

spectral region) was proportional to the light intensity over at least two decades. The trace was then photographed using a Polaroid camera with type 146L transparency film. Sample traces are shown in Chapters IV and V.

G. The Rapid-Scan System

The principal component of the spectrometer, shown schematically in Figure 6, is a Perkin-Elmer Model 108 Rapid Scan Monochromator. This instrument with appropriate prism is capable of scanning a selected spectral region between 0.2 and 10 μ, with from three to 150 scans per second. External controls permit selection both of the interval to be scanned and the center of scan. Different scanning speeds are obtained either by interchanging gears or with a two-speed switch. The spectral scan is produced by a modified double-pass Littrow system with a rotating tilted mirror. The slit is 12 mm high, with bilateral adjustment from zero to two mm, and the monochromator has an effective aperture of f/5. A photograph of the system is shown in Figure 7.

For the present application, a fused quartz prism was used, which can give a usable range with appropriate source and detector of from 0.2 to 2.5 μ. A sine sweep generator is incorporated into the monochromator, and should produce an output voltage proportional to the tilt angle of the nutating mirror to drive the horizontal input of an oscilloscope. The display produced should have a linearity

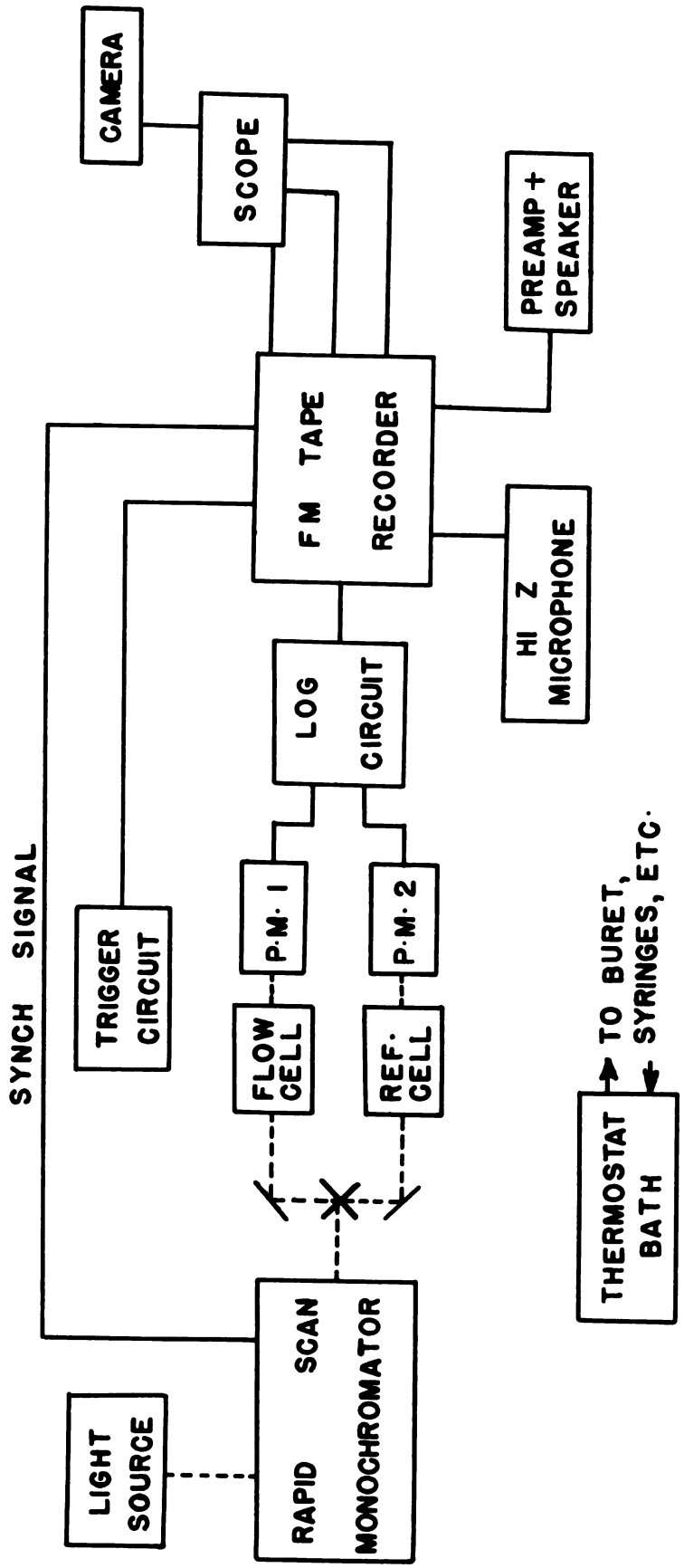

Figure 6. Schematic of rapid-scan system.

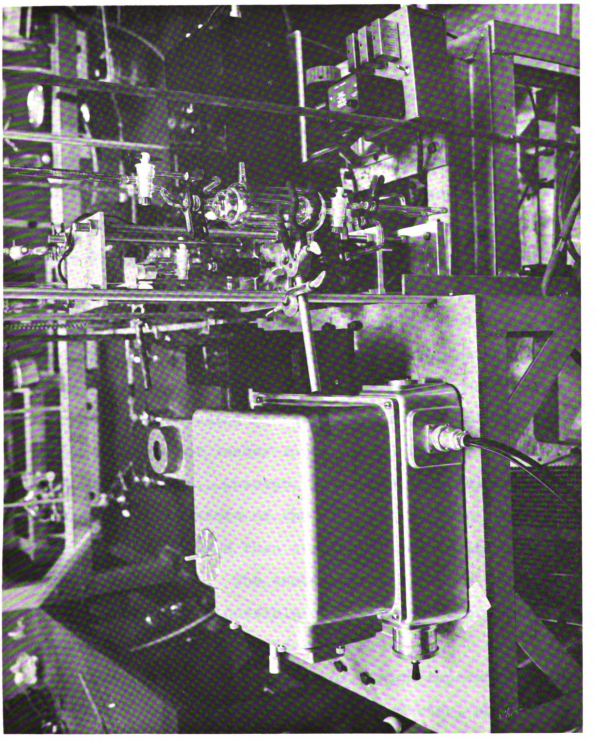

Figure 7. Photograph of rapid-scan system.

approaching the wavelength calibration curve of the prism, but, in fact, is non-linear because of a distorted sine output. Initial difficulties prevented superposition of the forward and reverse scans so that the signal could be used for triggering purposes only. Even this arrangement was not entirely satisfactory because noise on the synch signal caused random fluctuations in the triggering level. This led to an apparent shift in the spectral peaks under study.

The instrument has so far been used only over the range 0.4 to 1.1 μ. For this purpose a Bausch & Lamb source employing a tungsten-iodine lamp with a quartz envelope was used. As shown in Figure 6, the light after leaving the monochromator, impinges on a stacked mirror beam-splitter (from a Bausch & Lomb Spectronic 505 Spectrophotometer). The spherical focusing mirrors in this beam-splitter were replaced by two of longer focal length (98 mm) obtained from Karl Lambrecht Co., Chicago, Ill. The parallel beams are focused on the centers of the flow cell and on a reference cell, if desired, and then strike two photomultiplier tubes (RCA 6199 or 7102). The anode currents, which have been balanced as well as possible over the region of interest, are next fed into the log circuit.

The log circuit consists of a high impedance input amplifier, a dual logarithmic transconductor, an operational output amplifier, and a power supply. These components are available from Philbrick Researches, Inc. (Model nos. P25A,

PL1-P, P65AU, and PR-30C, respectively). This circuit produces an output voltage that is directly proportional to the logarithm of the ratio of the current from the reference phototube to that of the sample, and hence to the absorbance of the sample. The signal shape and absorbance are independent of photomultiplier voltage and of slit width, within limits set by low light intensity and spectral bandpass. The typical noise level for a well-resolved spectrum is five mv. peak-to-peak as measured on an oscilloscope.

The output voltage, adjusted to one volt per absorbance unit, is equal to absorbance from $\sim$ 0.01 to at least two absorbance units. Figure 8 shows a comparison of the spectrum of potassium permanganate taken with a Cary Model 14 Spectrophotometer and with our system. Figure 9 shows a test of Beer's Law for potassium permanganate in a one cm cell made with both the Cary 14 and with our apparatus. Also shown here are the results at higher concentration using a 1.0 mm capillary tube and the rapid-scan set-up. The capillary tube must be carefully masked in order to obtain reproducible results and avoid scattered light.

During a run, all pertinent data are stored on magnetic tape using an Ampex SP-300 FM Direct Recorder/Reproducer. Four channels are used as shown in Figure 6. The output of the log circuit, the synch signal from the monochromator, a triggering pulse, and an audio signal are each recorded on a separate channel and at least the first three by the same head.

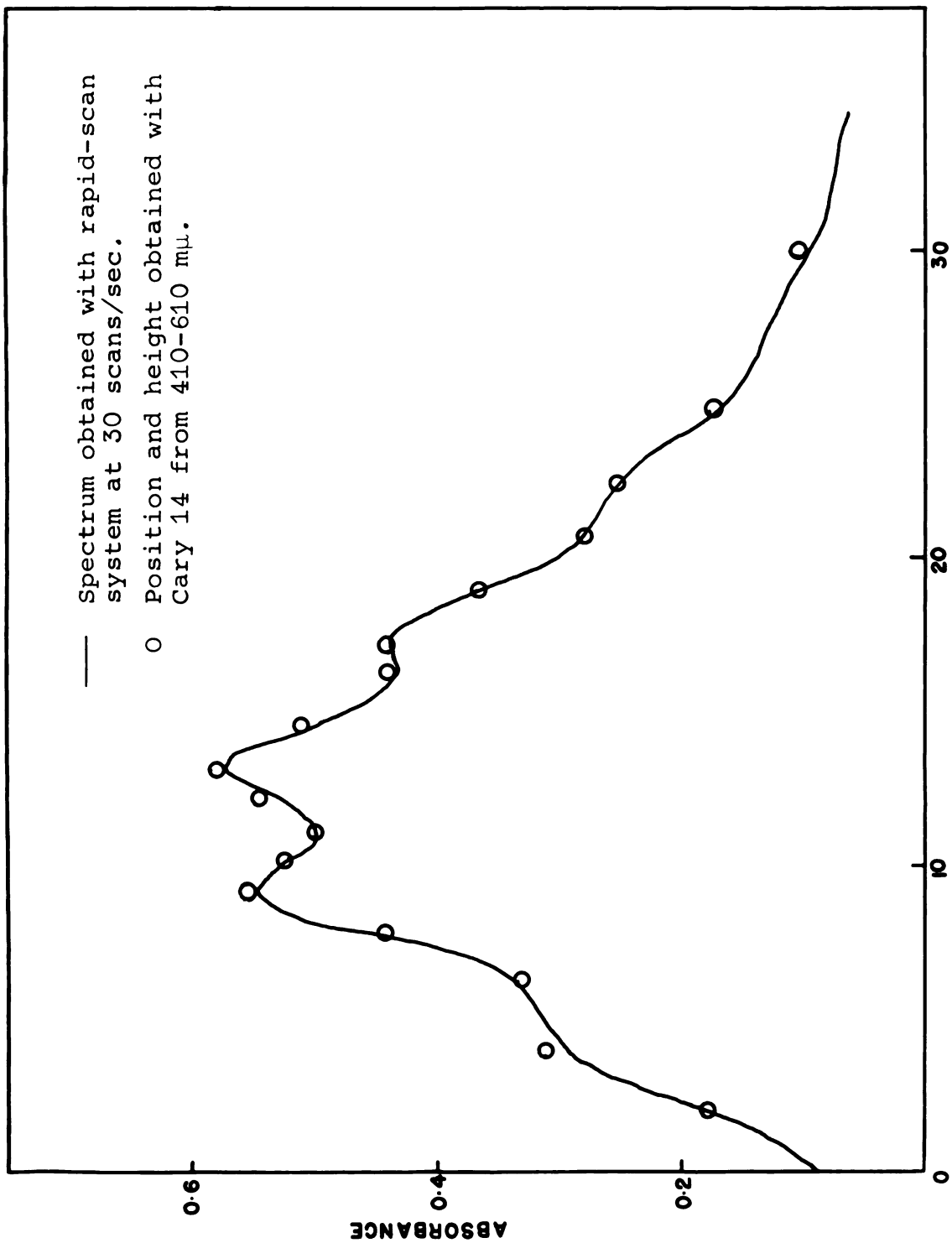

Figure 8. Comparison of a spectrum of potassium permanganate taken with a Cary Model 14 spectrophotometer and the rapid-scan system.

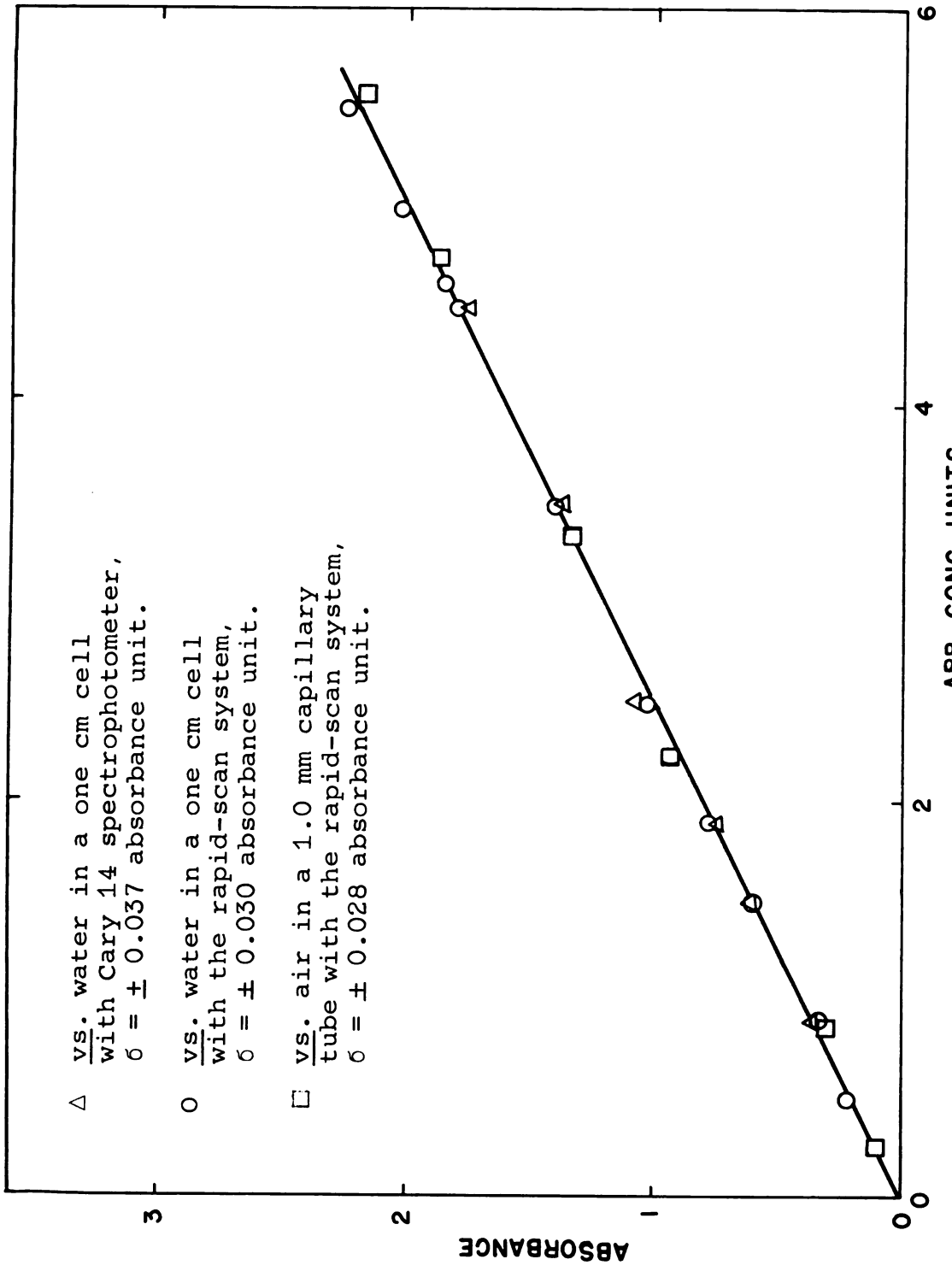

Figure 9. Test of Beer's Law for potassium permanganate at 525 mμ.

A cathode follower circuit must be used when recording the synch signal, if an undistorted signal is to be reproduced. If desired, the data may be monitored on an oscilloscope during recording.

The SP-300 in the FM mode has a frequency response of 0-2500 cps with noise level -35 db from one volt rms at 15 ips. At 7½ ips, the noise level is -38 db, but the frequency response is halved.

The recorded information is played back into a Tektronix Type 564 Storage Oscilloscope with types 2A63 Differential Amplifier and 3B4 Time Base plug-in units, and photographed. The channel containing the signal from the log circuit is played into the positive side of the differential amplifier, and a blank channel from the same head is played into the negative side to permit common-mode rejection of noise. The time base is triggered externally in the normal mode by the channel containing the synch signal from the monochromator. The 3B4 Time Base is equipped with a magnifier which permits selection of fractions of the display up to 1/50. In this way, every scan need not be examined. Examples of such spectra changing with time are shown in Figures 12a and b. The time between sweeps may be determined from the scanning rate of the monochromator. It should be pointed out that these spectra are sinusoidal rather than linear in wavenumber about the center of scan.

If a display of absorbance as a function of time at a given wavelength is desired, it may be obtained in either of two ways. From the data already stored on tape, the pulse may be used to trigger a slow sweep of the oscilloscope, such that the decay of the peak absorbance is displayed. This, as shown in Figure 12c, gives an envelope of absorbance with time at the wavelength corresponding to the highest spectral peak. With the second method it is necessary during a run to select the center of scan, minimize the wavelength interval scanned, and stop the motor. Then the output of the log circuit and triggering pulse are recorded, and the latter will trigger the scope during playback. This method is equivalent to that described for the fixed wavelength system (Sect. III-F). The transparencies were magnified using a photographic enlarger and traced on graph paper.

IV. RESULTS

A. Introduction

The reactions of all the alkali metals with water, cesium and rubidium with methanol, cesium with ethanol, and cesium with hydrogen chloride and ammonium bromide in ethylenediamine have been examined at fixed wavelength. Two runs were made of the reaction of cesium with water and one run of lithium with water in EDA using the rapid-scan system. These reactions were pseudo-first-order in metal, with solute concentration ten or more times greater than metal concentration. The overall rate constants and their order in solute were obtained by varying the solute concentration.

B. Alkali Metals + Water

1. At fixed wavelengths.

Cesium. The reaction of cesium with water in EDA was studied over a wide range of water concentrations, using several metal concentrations, and the results are given in Table III. Two rate constants were observed corresponding to the major absorbance changes, while in two runs at low water concentrations, a small initial absorbance change occurred with a faster rate constant varying from 38 to

Table III. Rate Constants for the Reaction of Cesium with Water in Ethylenediamine.*

Run 0.1 (Aug. 10, 1963). At room temp. Cesium conc. ~ 2.5×10^{-4} M (from absorbance).

Water Conc. (M)	λ(mμ)	k ($M^{-1}sec^{-1}$) fast	intermediate	slow
0.341	950	--	21.5, 20.3	5.14, 6.46, 5.65
0.0244	750	86, 200	--	--
0.0244	950	78	--	--
0.0244	1100	59.2, 100, 167	27.0, 24.9	--

Run 0.2 (Aug. 12, 1963). Apparatus broken on this run.

Run 0.3 (Aug. 16, 1963). At room temp. Cesium conc. = 1.4×10^{-4} M (by hydrogen analysis).

Water Conc. (M)	λ(mμ)	k ($M^{-1}sec^{-1}$) intermediate	slow
6.11	750	18.3, 24.9	5.2, 5.5
6.11	1100	24.1	6.2
0.341	950	21.2	4.1
0.341	1100	--	1,75, 5.9, 1.76
0.0244	750	10.8	6.4
0.0244	950	10.3	6.26
0.0244	1100	--	8.4, 5.9
4.0 with CsOH present	750	26, 26	11, 11
4.0 with CsOH present	950	22, 20	6.9, 6.6
4.0 with CsOH present	1100	14, 14, 31	11

Run 1.1 (Nov. 6, 1963). At room temp. Cesium conc. = 4.1×10^{-4} M (by hydrogen analysis).

Water Conc. (M)	λ(mμ)	k ($M^{-1}sec^{-1}$) fast	intermediate	slow
5.60	1100	--	28.3	10.7
5.60	950	--	28.0	10.5
5.60	750	--	28.6, 23.5	3.40, 5.43
0.670	1150	--	18.8	6.02, 2.91
0.670	950	--	10.1	2.91
0.670	750	--	6.79	2.42

*All concentrations are after mixing.

continued

Table III - Continued*

Run 1.1 - Continued

Water Conc. (M)	λ(mμ)	k ($M^{-1}sec^{-1}$) fast	intermediate	slow
0.0230	1100	56, 105	14.3, 15.5, 16.5	--
0.0230	950	82.5, 38.4	16.3, 15.0, 15.7	--
0.0230	750	--	17.1	--

Run 6.3 (Mar. 30, 1965). At 25.0 ± 0.2° C. Cesium conc. = 5.8×10^{-4} M (by hydrogen analysis).

Water Conc. (M)	λ(mμ)	k ($M^{-1}sec^{-1}$) intermediate	slow
1.78†	1100	6.8, 5.24	0.46, 1.15, 1.05, 1.41, 1.20, 1.22
0.928†	1100	4.38, 3.74	1.38, 0.54, 0.39, 0.72, 1.75
0.0728	1100	30.9, 16.7	4.29, 2.13, 2.64, 3.60

*All concentrations are after mixing.

†These solutions stood four months before use.

200 $M^{-1}sec^{-1}$. The intermediate and slow reactions are first-order in both metal and water, and show rates of 19.6 ± 4.9 and 5.3 ± 1.9 $M^{-1}sec^{-1}$, respectively. Unless specified otherwise, limits of error are given as average deviations from the mean. It appears, since only reducing species are present in the metal solutions, that these latter reactions are both simultaneous and competitive, and they were so treated. Figure 10a shows a typical oscilloscope trace and Figure 10b shows a plot of log Absorbance vs. time for this trace. No definite correlations of these reactions with wavelength could be made since the R and IR bands of the metal solution are extremely broad and overlap considerably (50). Since there are two competitive reactions, it would be expected that the initial absorbances would correlate with the appearance of the intermediate rate. At a given wavelength, for many traces that showed two rates, the initial absorbances had about the same values. In other traces at the same wavelength when there was only one rate, initial absorbances were about those corresponding to only the intermediate or the slow rate, depending upon which one was observed. Unfortunately these correlations did not hold in a number of cases, which is probably due to partial decomposition of the cesium solutions in the syringe prior to pushing, and resulting shifts in equilibria (52).

Rubidium and potassium. Rubidium and potassium solutions were studied using a single run for each metal and the

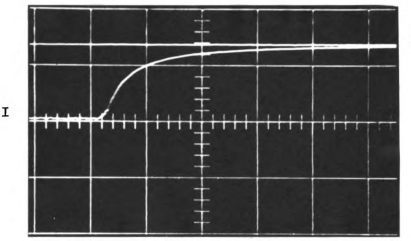

Time (20 msec/division)

Figure 10a. Typical oscilloscope trace for the reaction of cesium with water in ethylenediamine showing two rates.

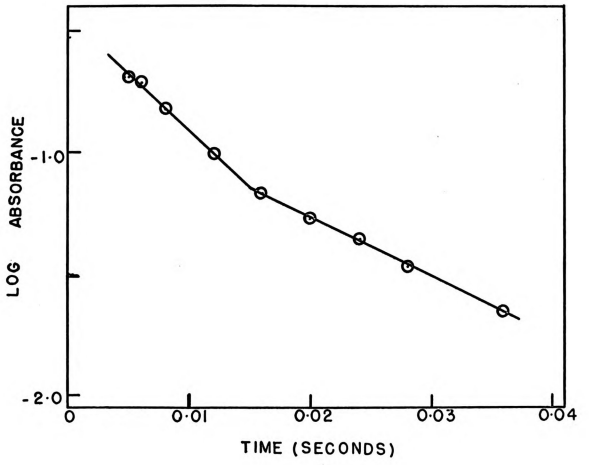

Figure 10b. Plot of log Absorbance vs. time for this trace.

results are summarized in Table IV. These results are similar to those using cesium. The reaction of rubidium with water gives rate constants of 157, 12.6 ± 2.8, and 3.3 ± 1.0 $M^{-1}sec^{-1}$, and potassium + water yields rates of 14.8 ± 2.7 and 3.9 ± 0.9 $M^{-1}sec^{-1}$.

Sodium. Three runs were made with solutions of sodium in EDA and the results are presented in Table V. The reaction of sodium with water in EDA is also first-order in metal absorbance, and except in a few instances, shows but a single rate. A plot of log κ (where κ is the pseudo-first-order rate constant) vs. log (water concentration) is shown in Figure 11. The solid line was fitted to the data by the method of least squares using a cubic equation. This line gave the best fit for polynomials of degree one through four. The single point obtained by Dewald (11) is also shown, and is in agreement with these results.

Lithium. The reaction of lithium with water was studied in three runs and the results are displayed in Table VI. In Run 2.2, lithium prepared by evaporation of a metal-ammonia solution was used, while in the other runs, lithium in a side-arm was used (Sect. III-B). The absorbance at 700 mμ was very low relative to that at 1100 mμ (for Run 2.2) which would lead to the assignment of the faster rates to the IR species. Run 6.2, however, consisted of a very dilute solution showing no IR band, and resulted in a single rate

Table IV. Rate Constants for the Reactions of Rubidium and Potassium with Water in Ethylenediamine at Room Temperature.*

Run 1.2 (Nov. 9, 1963) Rubidium conc. = 1.34×10^{-3} M(by hydrogen analysis).

Water Conc. (M)	λ(mμ)	k($M^{-1}sec^{-1}$) fast	intermediate	slow
5.60	750	--	11.1	3.84
5.60	1100	--	4.25	1.16
0.580	750	--	10.9	--
0.580	1100	--	--	4.96,3.52
0.0230	750	182, 89.6	14.2	--
0.0230	900	199	17.9	--
0.0230	1100	--	8.91	2.87

Run 3.1 (May 21, 1964). Potassium conc. = 1.15×10^{-4} M (by hydrogen analysis).

Water Conc. (M)	λ(mμ)	k($M^{-1}sec^{-1}$) intermediate	slow
4.06	700	17.2, 17.2	4.82, 4.82
4.06	850	16.7	4.18
4.06	950	17.7, 14.6, 16.7 12.5	4.18, 4.19, 4.44, 4.32
0.590	700	--	3.03
0.590	800	15.5, 20.9	3.79, 4.54, 3.20
0.590	1110	11.7, 10.7, 11.5, 13.0, 10.7	1.89, 2.44, 2.44, 6.50

*All concentrations are after mixing.

Table V. Rate Constants for the Reaction of Sodium with Water in Ethylenediamine.*

Run 2.1 (Mar. 7, 1964). At room temp. Sodium conc. = 3.3 x 10^{-4} M (by hydrogen analysis).

Water Conc. (M)	λ(mμ)	κ(sec^{-1})
4.07	750	6.54, 8.80, 8.15, 8.20, 7.15, 8.40
4.07	850	6.25
2.02	750	1.62, 1.16, 1.08, 1.08
0.589	700	0.336
0.589	750	0.212, 0.224
0.024	700	0.053

Run 5.2 (Oct. 26, 1964). At 25.0 ± 0.2° C. Sodium conc. ~1 x 10^{-4} M (from absorbance).

Water Conc. (M)	λ(mμ)	κ(sec^{-1}) I†	κ(sec^{-1}) II
3.01	730	10.7, 21.6	2.04, 6.52, 2.40, 1.70, 1.54, 3.33
0.295	730	--	0.0936, 0.0779
0.0372	730	--	0.0647, 0.0666

Run 6.1 (Mar. 11, 1965). At 25.0 ± 0.2° C. Sodium conc. = 1.4 x 10^{-4} M (by hydrogen analysis).

Water Conc. (M)	λ(mμ)	κ(sec^{-1}) I†	κ(sec^{-1}) II
1.78	700	13.2	2.36, 2.00, 1.40, 2.40, 1.00
0.850	700	--	1.00, 0.350, 0.320, 1.13
0.248	700	1.54	0.292, 0.433, 0.032, 0.533
0.0728	700	1.25, 1.22	0.245, 0.117, 0.117
0.0728	730	1.48, 1.56	0.27, 0.20

*All concentrations are after mixing.

†Cf. Sect. V-E.

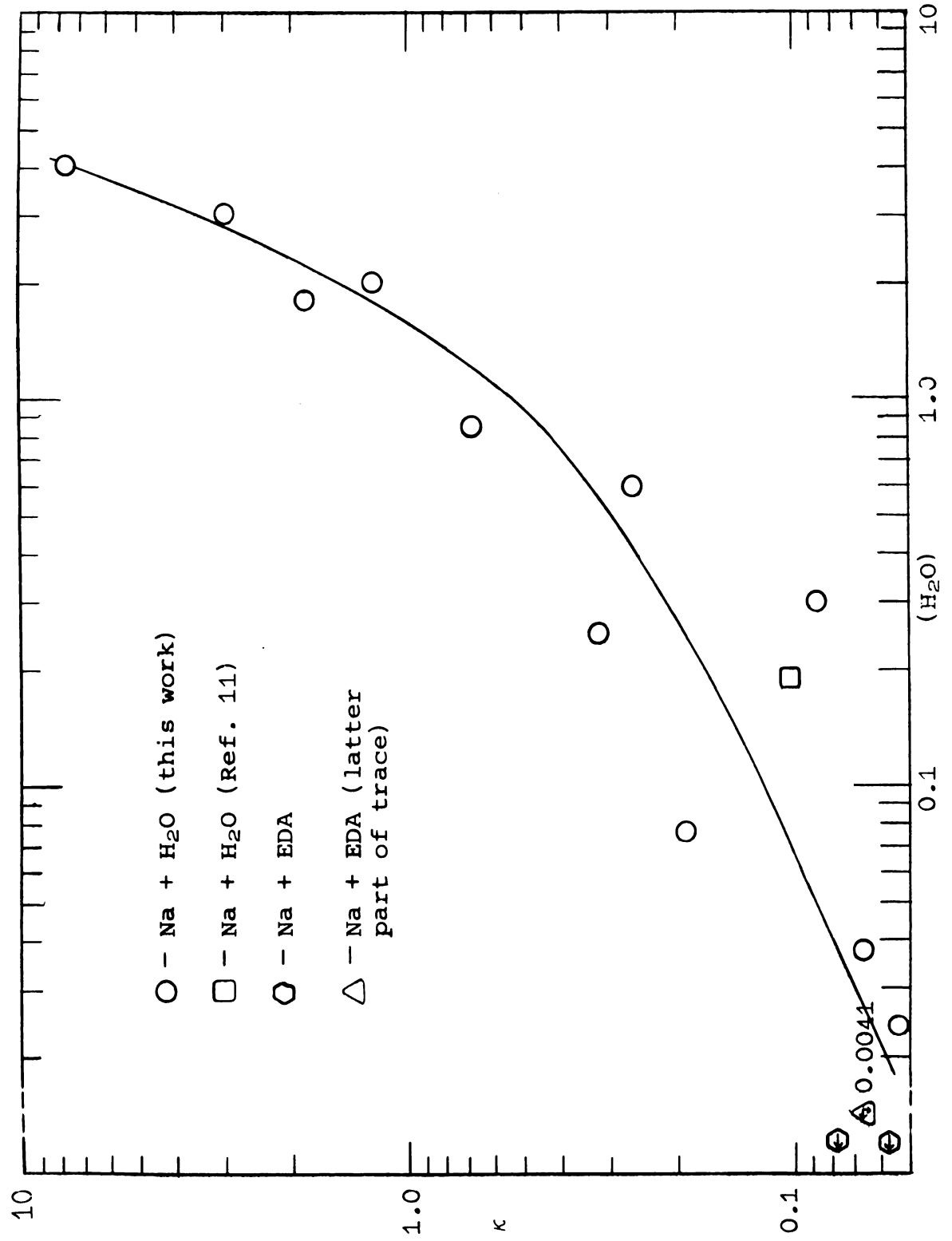

Figure 11. Log κ vs. log (water concentration) for the reaction of sodium with water in ethylenediamine.

Table VI. Rate Constants for the Reaction of Lithium with Water in Ethylenediamine.*

Run 2.2 (Mar. 12, 1964). At room temp. Lithium conc. ~ 2×10^{-4} M (from absorbance).

Water Conc. (M)	λ(mμ)	k($M^{-1}sec^{-1}$) fast	intermediate	slow
0.0238	700	--	--	9.07, 9.07
0.0238	1100	91.6, 69.4, 109, 102, 71.5	30.3, 50.5, 30.0, 19.2, 50.5	7.26, 10.9, 10.2

Run 5.3 (Nov. 6, 1964). At 25.0 ± 0.2° C. Lithium conc. ~ 1×10^{-3} (from absorbance).

Water Conc. (M)	λ(mμ)	k($M^{-1}sec^{-1}$) fast	intermediate	slow
3.01	720	--	30.4, 14.1	4.25, 3.79, 5.65
3.01	1100	--	10.3, 16.6	2.81, 3.04, 3.32, 2.89
1.39	1100	--	23.8, 28.2	8.63, 2.50, 3.07
0.295	720	94.9, 112	--	1.42
0.295	1100	92.2	--	1.42, 1.08
0.0372	715	193, 254	38.4, 26.9	5.86, 5.50, 5,16
0.0372	1100	91.1, 64.5, 215	40.3, 61.1	4.30, 4.22, 7.53, 8.71 4.30

Run 6.2 (Mar. 22, 1965). At 25.0 ± 0.2° C. Lithium conc. ~ 10^{-5} M (from absorbance).

Water Conc. (M)	λ(mμ)	k ($M^{-1}sec^{-1}$)
0.0728	700	32.4
0.0728	650	37.8, 25.5, 19.2, 33.7

*All concentrations are after mixing.

constant of 29.7 ± 5.9 $M^{-1}sec^{-1}$ obtained by following the decay of the 660 mμ absorbance. The third run, Run 5.3, yielded up to three rate constants with values of 140, 27.3 ± 6.9, and 4.3 ± 1.6 $M^{-1}sec^{-1}$.

2. With rapid-scan system.

Cesium. Three runs were made using the rapid-scan system--two with cesium + water and one with lithium + water. The results of these runs are given in Table VII. For Run 7.1, a dilute solution of cesium in EDA was prepared. Picture no. 4, obtained from playback of the tape recorder, is shown in Figure 12a and Figure 13 gives plots of ln Absorbance vs. time for this trace made at different wavelengths. Agreement among rate constants for a given trace is reasonable, and the differences in values between traces probably result from an inability to correct the rates for the presence of the second slower rate. Analysis of such traces was made more difficult by the lack of triggering stability, and by the fact that the relative errors increase near the bottom of the trace. Also to be considered is the decreased sensitivity of the spectrometer for large spectral scans through a one mm capillary tube, since the photomultipliers were operating in a region of poor sensitivity at low light intensity. Again, decomposition and shifts in equilibria may play an important role. The upper limit of the scanning rate, 6.7 msec/scan, made detection of the intermediate rate difficult at high water concentrations ($\tau_{\frac{1}{2}} \sim 9$ msec). The presence of the intermediate rate resulted

Table VII. Rate Constants for the Reactions of Cesium with Water and Lithium with Water using the Rapid-Scan System at 25.0 ± 0.2° C.*

Run 7.1 (July 21, 1965). Cesium conc. = 4.0 x 10^{-4} M (by hydrogen analysis).

Pict. No.	Water Conc. (M)	~λ(mμ) - k ($M^{-1}sec^{-1}$)
4	0.0369	1150-14.9; 1080-12.9; 900-13.5; 650-14.8
5	0.0369	1150-9.22; 1060-9.90; 900-7.50
6	0.380	1100-23.6; 1050-21.2; 950-20.4
8	0.380	1150-14.5; 1050-11.7; 850-8.43
9	0.380	1100-10.4; 900-18.7
10	0.380	1100-10.9; 1050-15.0; 900-11.2
11	0.380	1125-20.2; 1050-24.9; 900-18.6
12	3.18	1100-2.28; 1000-1.86; 800-5.17, 1.73
14	3.18	1050-12.0, 2.92
15	1.73	1100-2.28; 1050-2.60; 975-2.12
16	1.73	1100-1.35; 950-1.40
17	1.73	1100-4.10, 0.93; 950-3.20, 1.06

Run 7.2 (July 27, 1965). Cesium conc. ~ 2 x 10^{-3} M (from absorbance).

Pict. No.	Water Conc. (M)	~λ(mμ) - k ($M^{-1}sec^{-1}$)
8 left	0.0369	1150-4.94; 1050-24.9, 3.20
8 right	0.0369	1150-26.1, 3.26; 1050-9.46; 850-4.62
9	0.0369	1150-6.26; 1050-5.98; 850-6.23
10	0.0369	1200-4.16; 1050-2.87; 875-5.13
11	0.380	1100-12.8, 2.27; 900-2.98
12	0.380	1150-5.05; 1050-4.56; 850-3.96
13	0.380	1150-4.08; 1075-5.18; 1000-4.68
14 left	0.380	1100-5.42; 900-5.11
14 right	0.380	1100-12.6, 2.05; 900-5.27
15	3.18	1050-13.1

*All concentrations are after mixing.

continued

Table VII - Continued*

Run 7.3 (July 30, 1965). Lithium conc. ~4 x 10^{-3} M (from absorbance).

Pict. No.	Water Conc. (M)	~λ(mμ) - k ($M^{-1}sec^{-1}$)
1	0.0369	1200-32.1, 8.23; 1050-27.4, 7.41
2	0.0369	1200-15.5; 1050-31.5, 8.62
3	0.0369	1200-40.7, 10.3; 1000-32.0, 8.18
4	0.0369	1200-74.6, 18.4; 1050-90.9, 13.6; 850-39.7
5	0.0369	1050-38.8, 9.21
7	0.380	1150-85.8; 750-73.0
8	0.380	1050-91.1
11	0.380	1050-111, 37.5
13	0.380	1050-134, 62.2
15	3.18	1050-fast rate, 11.8, 3.99

*All concentrations are after mixing.

Abs.

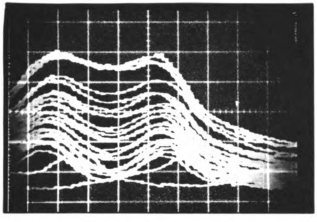

0.212 sec/scan

Figure 12a. Typical trace for the reaction of cesium with water taken with the rapid-scan system.

Abs.

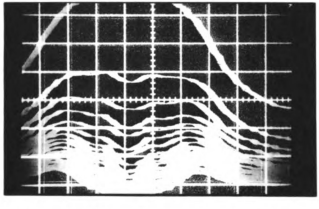

0.53 sec/scan

Figure 12b. Typical trace for the reaction of lithium with water taken with the rapid-scan system.

Abs.

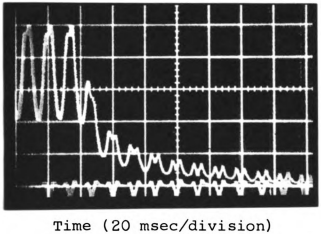

Time (20 msec/division)

Figure 12c. Slow oscilloscope sweep for the reaction of lithium with water taken with the rapid-scan system.

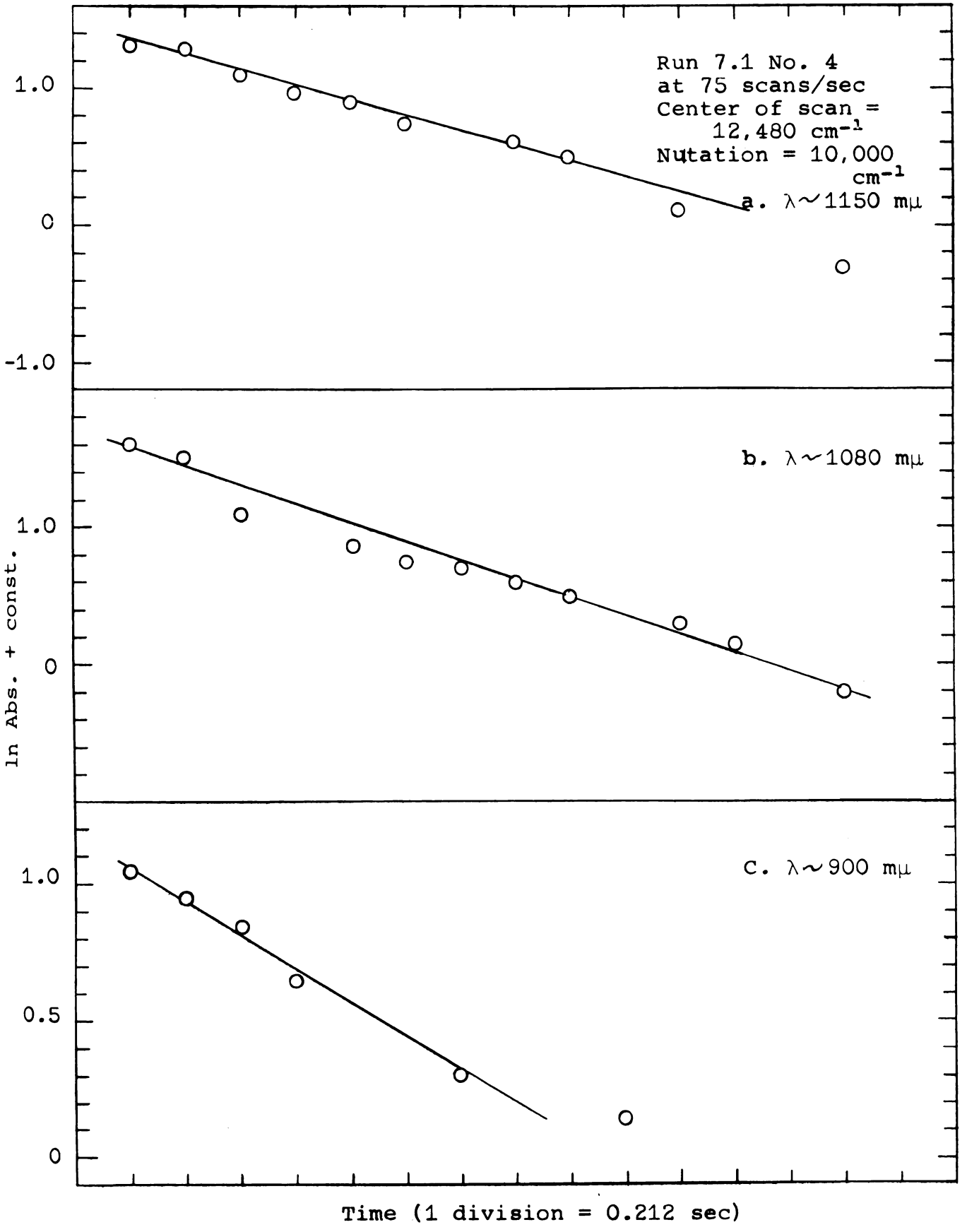

Figure 13. Plots of ln Absorbance vs. time for Fig. 12a.

in a large decrease in absorbance between mixing and the first scan after flow had been stopped. The results of Run 7.2, in which a more concentrated cesium solution was employed, were similar to those of 7.1. Analysis of spectral shape for these runs will be discussed in Chapter V.

Lithium. A run with lithium, prepared in the dry box, was carried out using the rapid-scan system. Figure 12b shows the trace for picture no. 1 of Run 7.3, and plots of ln Absorbance vs. time for this trace are presented in Figure 14. Figure 12c shows the decay of peak absorbance with time for picture no. 15. The oscilloscope sweep rate is slow enough to give a number of complete spectra in a single sweep resulting in an envelope whose appearance is similar to the usual decay curves at fixed wavelength. A plot of ln Absorbance vs. time for this trace is presented in Figure 15. The spectrum of this lithium solution shows primarily the IR band, and yet these kinetic studies apparently yield three distinct rate constants. These results agree with those obtained earlier at fixed wavelength.

C. Rubidium and Cesium + Methanol

The reactions of rubidium and cesium with methanol in ethylenediamine were studied at fixed wavelengths, and the results are presented in Table VIII. While reaction times are comparable to those observed in the water reactions, several marked differences are apparent. In some cases,

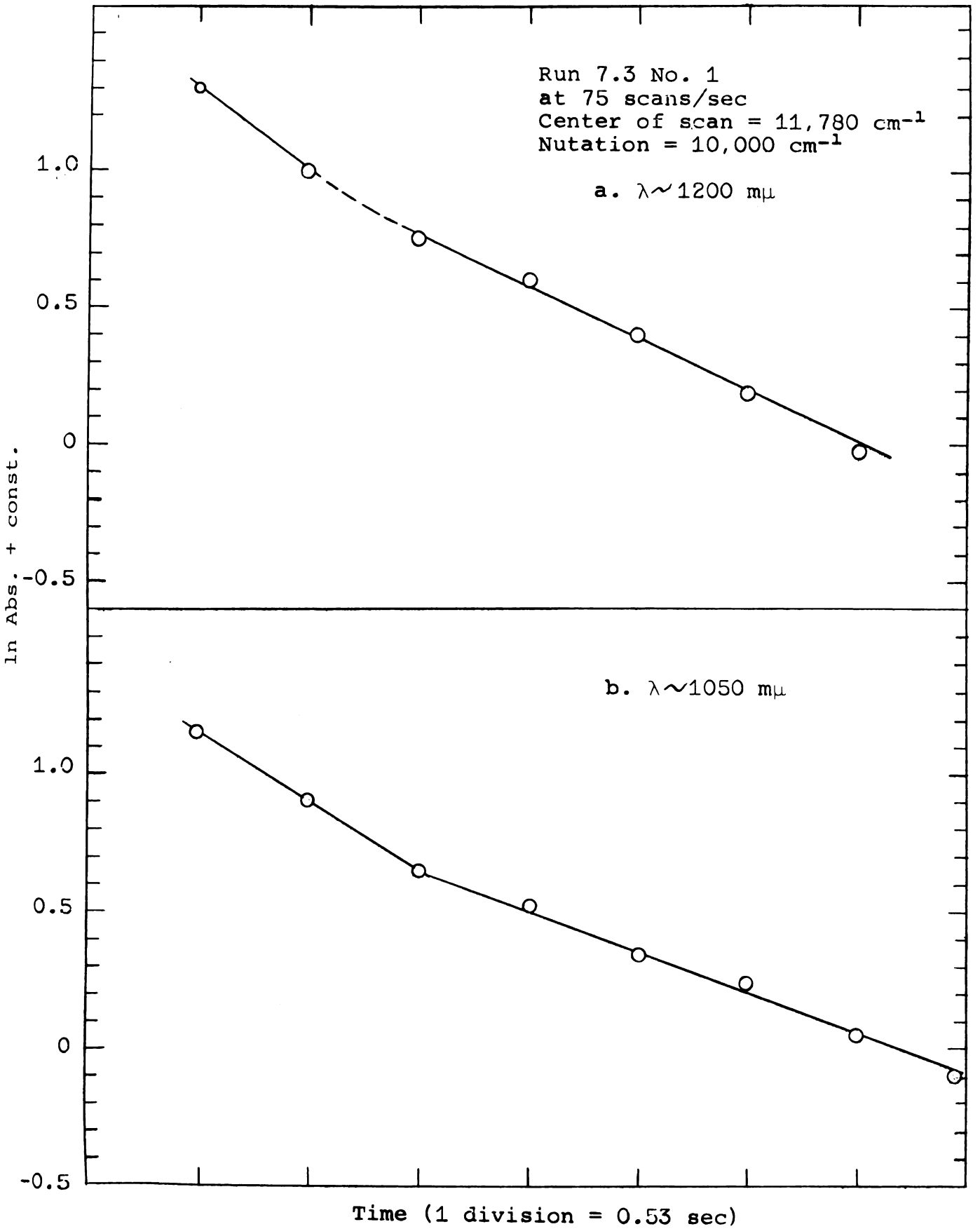

Figure 14. Plots of ln Absorbance vs. time for Fig. 12b.

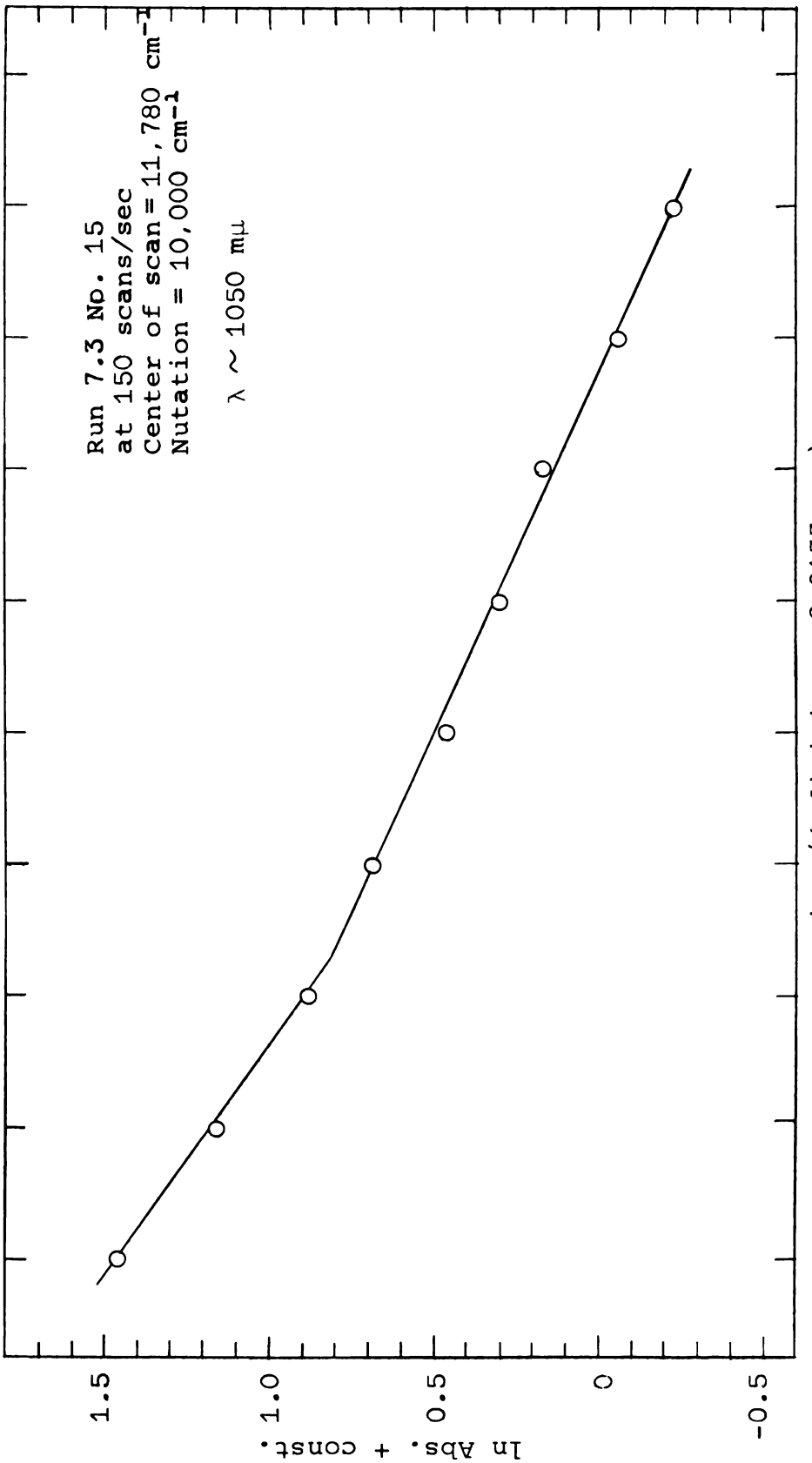

Figure 15. Plot of ln Absorbance vs. time for Fig. 12c.

Table VIII. Rate Constants for the Reaction of Rubidium and Cesium with Methanol in Ethylenediamine.*

Run 1.1 (Nov. 6, 1963). At room temp. Cesium conc. = 4.1×10^{-4} M (by hydrogen analysis).

Methanol Conc.(M)	λ(mμ)	k ($M^{-1}sec^{-1}$) II	III	IV
0.767	750	60.0	11.6	5.50
0.767	950	--	10.4, 10.7	4.26, 6.78, 7.38, 7.20, 4.90, 5.95, 3.90

Run 1.2 (Nov. 9, 1963). At room temp. Rubidium conc. = 1.3×10^{-3} M (by hydrogen analysis).

Methanol Conc.(M)	λ(mμ)	k ($M^{-1}sec^{-1}$)
0.767	750	6.03, 7.71
0.767	1100	9.84, 1.56

Run 4.2 (Sept. 21, 1964). At 25.0 ± 0.2° C. Cesium conc. = 5.1×10^{-4} M (by hydrogen analysis).

Methanol Conc.(M)	λ(mμ)	k ($M^{-1}sec^{-1}$) I	II	III	IV
0.105	950	610, 476, 419	70.5	19.4, 12.2, 29.1, 15.2, 14.5	--
0.536	950	---	50.6, 61.6, 74.6	18.7, 10.6, 12.4	4.98
1.95	950	192, 214, 150	--	--	--

Run 5.1 (Sept. 25, 1964). At 25.0 ± 0.2° C. Cesium conc. = 4.1×10^{-4} M (by hydrogen analysis).

Methanol Conc.(M)	λ(mμ)	k ($M^{-1}sec^{-1}$) I	II	III	IV
0.105	850	381, 168	--	12.0, 14.7	--
0.105	950	430	67.7, 61.2	13.9	--
0.105	1100	229, 100	--	16.2, 24.2, 22.3, 19, 14.3	--
0.353	1100	--	81.6, 86.1, 61.2, 65.7	13.6, 13.0, 10.6	8.50, 7.08, 3.88, 4.39
0.531(1 trace)	850	--	74.6	20.0	7.89
0.536	1100	--	--	9.33	5.49, 7.01, 5.88

*All concentrations are after mixing.

using cesium solutions, more than one rate was observed in a given trace, but the constants were not reproducible. In Table VIII, the second-order rate constants obtained have been arranged into four groups depending upon magnitude. More striking was the fact that the shapes of the traces themselves differed from picture to picture, and in some cases showed what seems to be an absorbing intermediate. Such a trace is displayed in Figure 16a and a plot of ln Absorbance vs. time for this trace is given in Figure 17a.

D. Cesium + Ethanol

Two runs were made with solutions of cesium and ethanol in ethylenediamine. The results of these runs are compiled in Table IX. Most traces were similar in appearance to those obtained with water (see Fig. 16b), but some pictures, Run 4.1 nos. 9-15, showed behavior like that observed with methanol (see Fig. 16c). Plots of ln Absorbance vs. time for the traces in Figures 16b and c are given in Figures 17b and c, respectively. The reaction is clearly first-order in metal absorbance, but no definite order in ethanol can be assigned. Competitive processes and/or reaction intermediates could account for this difficulty.

E. Cesium + Ethylenediammonium and Ammonium Ions

Hydrogen chloride was reacted with cesium in EDA and several traces were obtained. The results of these pushes

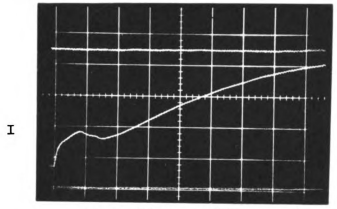

Time (0.2 sec/division)

Figure 16a. Typical trace for the reaction of cesium with methanol in ethylenediamine.

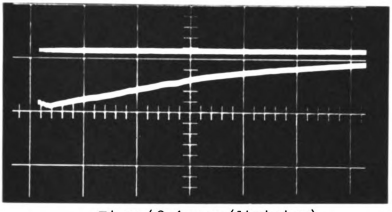

Time (0.1 sec/division)

Figure 16b. Typical trace for the reaction of cesium with ethanol in ethylenediamine (no intermediate).

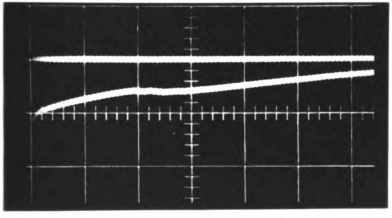

Time (0.2 sec/division)

Figure 16c. Typical trace for the reaction of cesium with ethanol in ethylenediamine (intermediate present).

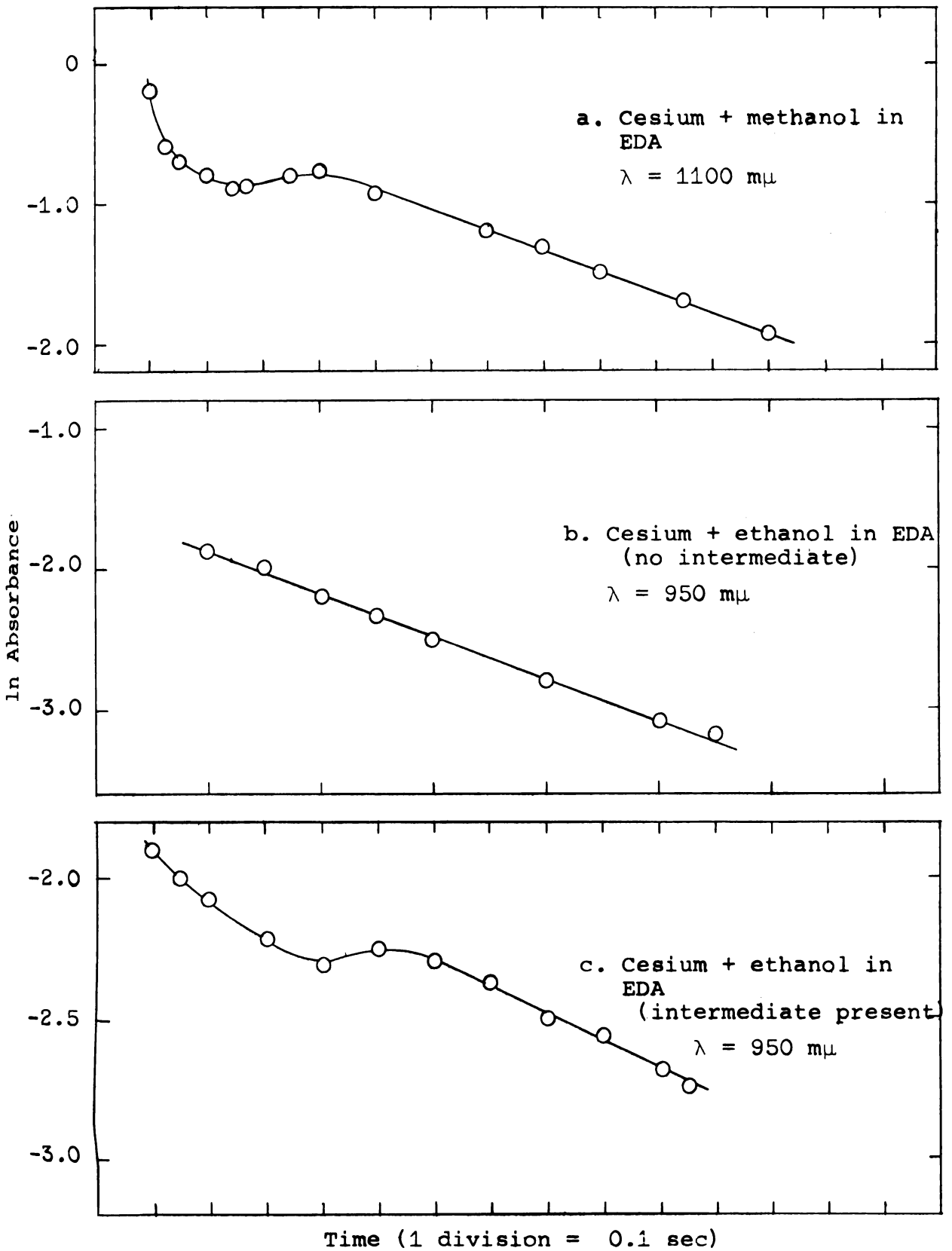

Figure 17. Plots of ln Absorbance vs. time for the traces in Fig. 16.

Table IX. Rate Constants for the Reaction of Cesium with Ethanol in Ethylenediamine.*

Run 3.2 (June 9, 1964). At room temp. Cesium conc. = 4×10^{-4} M (from absorbance).

Trace No.	λ(mμ)	Ethanol Conc. (M)	κ(sec^{-1})
3	900	0.117	3.10, 1.60
4	900	0.117	3.10, 1.60
6	1100	0.117	2.70, 1.75
7	700	0.117	1.75
8	950	0.117	1.90
9	950	1.04	3.90
10	950	1.04	1.50
13	950	1.04	5.10
14	950	1.04	5.00
16	950	0.504	4.30
17	950	0.504	2.80
18	950	0.504	2.90
19	950	0.504	2.20
21	950	0.504	3.20
22	950	0.504	2.00
23	950	1.61	4.50
24	950	1.61	8.50
27	950	1.61	4.10

Run 4.1 (Aug. 12, 1964). At 25.0 ± 0.2° C. Cesium conc. = 1.8×10^{-3} M (by hydrogen analysis) and λ = 950 mμ.

Trace No.	Ethanol Conc. (M)	κ(sec^{-1})
5	1.04	13.7
6	1.04	5.95
8	1.04	5.30
9	0.521	1.94
10	0.521	1.67
11	0.521	1.44
12	0.521	1.57
13	0.521	1.70, 1.30
14	0.521	1.48, 1.14
15	0.521	2.00, 0.527
16	1.61	38.2, 17.6
17	1.61	27.5, 14.3
18	1.61	24.1
19	1.61	20.0
20	1.61	25.6
21	0.537	1.47
22	0.537	1.50
23	0.537	1.50
24	0.537	7.50, 1.57
25	0.537	2.65

*All concentrations are after mixing.

are given in Table X. A rate constant of $1.7 \pm 0.2 \times 10^5$ $M^{-1}sec^{-1}$ was observed. The reaction of ammonium bromide with cesium in EDA was too fast to be followed by the flow method for the two concentrations employed, but a lower limit of 3×10^6 $M^{-1}sec^{-1}$ could be calculated for the rate constant of this reaction.

Table X. Rate Constants for the Reactions of Cesium with Ethylenediammonium Chloride and Ammonium Bromide in Ethylenediamine.*

Run 5.1 (Sept. 25, 1964). At 25.0 ± 0.2° C. Cesium conc. = 4.1×10^{-4} M (by hydrogen analysis).

$EDAH^+$ Conc. (M)	λ(mμ)	k ($M^{-1}sec^{-1}$)
1.0×10^{-3}	1100	$(1.7, 2.0, 1.5) \times 10^5$

Run 6.3 (Mar. 30, 1965). At 25.0 ± 0.2° C. Cesium conc. = 5.8×10^{-4} M (by hydrogen analysis).

NH_4^+ Conc. (M)	λ(mμ)	$\tau_{\frac{1}{2}}$ (msec)	k ($M^{-1}sec^{-1}$)
5.5×10^{-4}	1100	< 2	$> 8 \times 10^5$
5×10^{-5}	1100	< 2	$> 3 \times 10^6$

*All concentrations are after mixing.

V. DISCUSSION

A. Introduction

The reaction of dilute solutions of cesium with water in ethylenediamine was studied by Dewald et al. (11,12) who obtained a rate constant of 24.7 ± 1.5 $M^{-1}sec^{-1}$. On the basis of optical absorption spectra (50) and other evidence (51,52), it was assumed that this reaction was that of the solvated electron as well as loosely-bound electrostatic aggregates of electrons and cations with water. This permitted correlation with the results of aqueous radiation chemistry.

Since solute concentration was in excess, all reactions studied in this investigation appeared to be pseudo-first-order in metal absorbance, so that

$$-d(Abs.)/dt = \kappa \qquad (1)$$

then

$$(Abs.) = (Abs.)_o \exp(-\kappa t) \qquad (2)$$

or

$$\ln(Abs.) = -\kappa t + \ln(Abs.)_o \qquad (3)$$

In these equations, $\kappa = k(R)^n$, where k is the overall rate constant and n is the order with respect to the reactant in excess. A plot of log κ vs. log (R) will give both k and n.

For a large number of traces, a plot of ln (Abs.) *vs.* time yielded two straight line portions with different slopes. Such cases were treated as simultaneous, competitive reactions in the following manner: Letting

$$A \xrightarrow{\kappa_a} \text{products} \tag{4}$$

and

$$B \xrightarrow{\kappa_b} \text{products} \tag{5}$$

then

$$A = A_o \exp(-\kappa_a t) \tag{6}$$

and

$$B = B_o \exp(-\kappa_a t) \tag{7}$$

so

$$\ln(A+B) = \ln[A_o \exp(-\kappa_a t) + B_o \exp(-\kappa_b t)] \tag{8}$$

Next,

$$\frac{d\ln(A+B)}{dt} = \frac{-\kappa_a A_o \exp(-\kappa_a t) - \kappa_b B_o \exp(-\kappa_b t)}{A_o \exp(-\kappa_a t) + B_o \exp(-\kappa_b t)} \tag{9}$$

At t = 0,

$$\frac{d\ln(A+B)}{dt} = \frac{-\kappa_a A_o - \kappa_b B_o}{A_o + B_o} \equiv -\kappa_a^{app} \tag{10}$$

which simplifies to

$$\kappa_a^{true} = \kappa_a^{app} + \frac{B_o}{A_o}(\kappa_a^{app} - \kappa_b) \tag{11}$$

where κ_a^{app} is the observed higher rate constant, κ_b is the lower rate constant, A_o and B_o are the initial absorbances of species A and B, respectively, and κ_a^{true} is the corrected value of κ_a. In this derivation it has been assumed that Beer's Law is valid for species A and B, noting that even if

the extinction coefficients are different, the final expression is unchanged.

For the most part, the traces obtained with the fixed-wavelength stopped-flow apparatus were of excellent quality. Good first-order kinetic plots were obtained from them. Often the traces obtained in subsequent pushes under the same conditions could be superimposed exactly. In spite of this, over the course of a run there was an abnormal amount of scatter in the rate constants obtained. Analysis in terms of two reactions, as described above, improved the precision significantly, but the deviations were still much larger than the expected instrumental error. The difficulty probably lies with the solutions themselves since they are somewhat unstable and very sensitive to impurities which could lead to partial decomposition and shifts in the various equilibria.

B. Alkali Metals + Water

1. Cesium, rubidium, and potassium. From the results at fixed wavelengths, for the reaction of cesium with water in EDA, it was felt that the second-order rate constant of about 20 $M^{-1}sec^{-1}$ was compatible with the previous assignment to the solvated electron (and loose aggregates). If this were the case, then the slower reaction might be assigned to the reaction of the R band species. Figures 18 and 19 show plots D/D_{1100} (D = absorbance) vs. wavelength

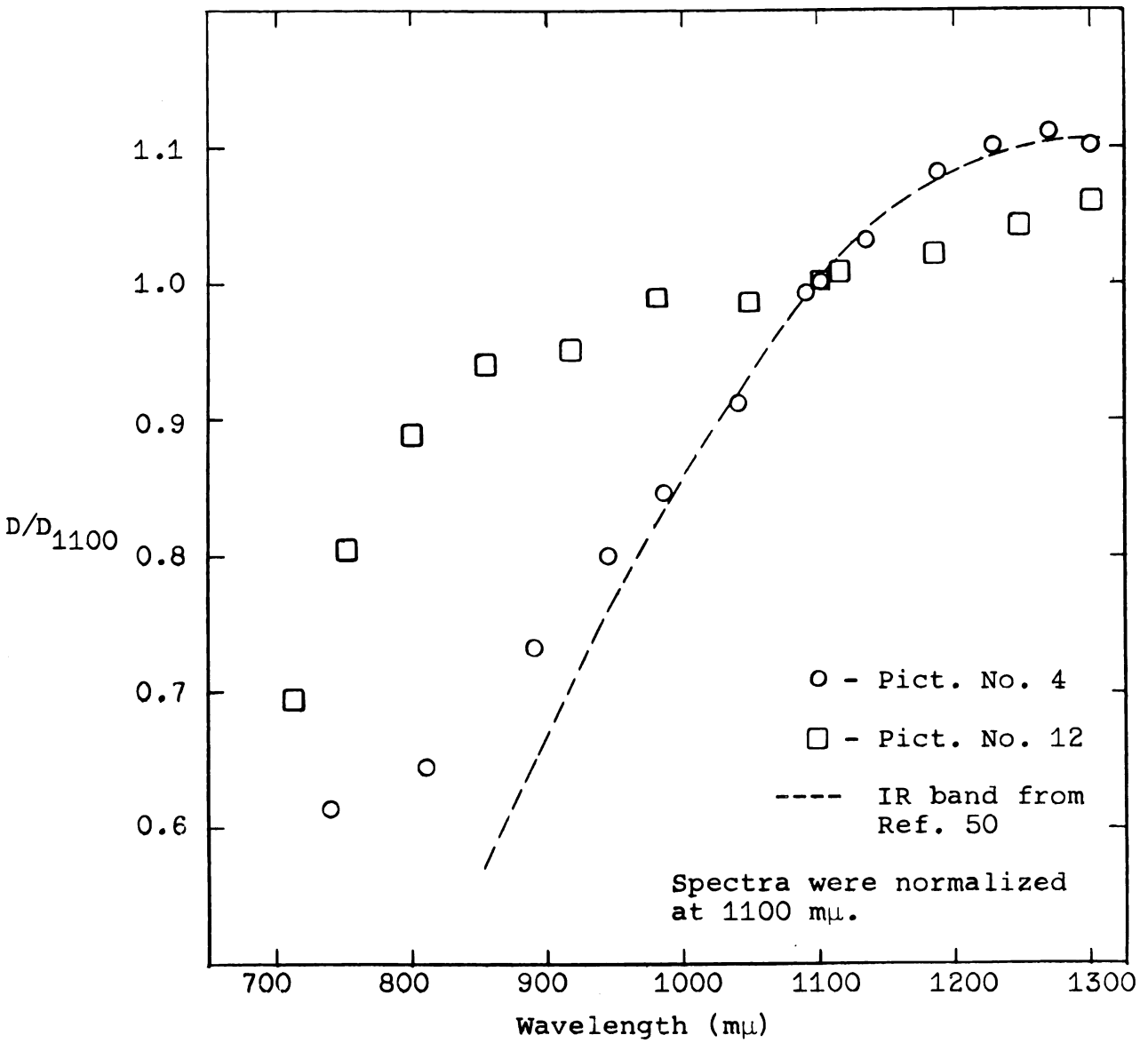

Figure 18. Comparison of the spectral shapes for typical traces of Run 7.1 with that of Dewald and Dye (50).

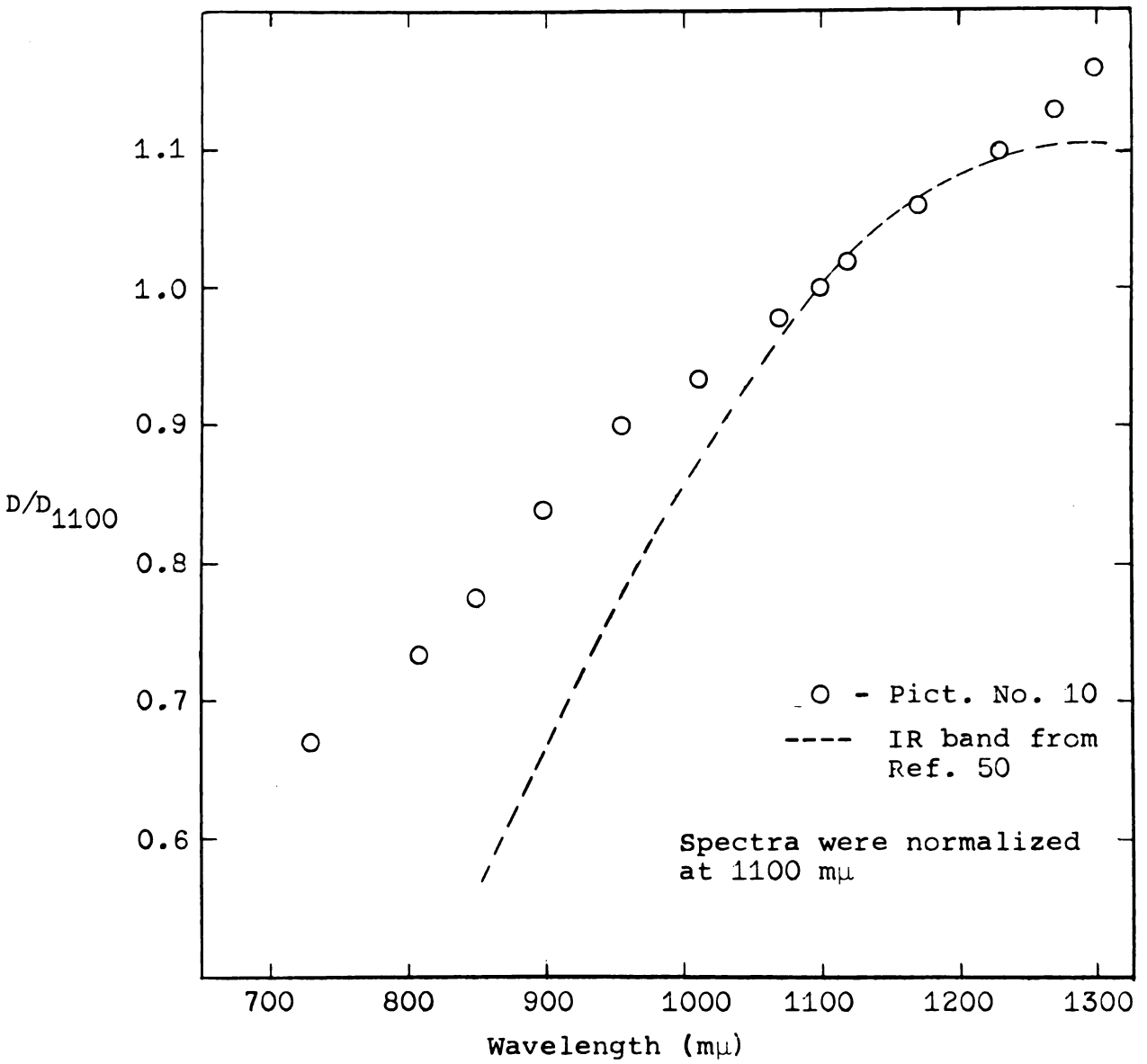

Figure 19. Comparison of the spectral shape of a typical trace of Run 7.2 with that of Dewald and Dye (50).

for typical traces from Runs 7.1 and 7.2, respectively, compared to the spectral results of Dewald and Dye (50). The shape of the rapid-scan spectrum in Figure 18, corresponding to Run 7.1, picture no. 4, is close to that of Dewald and Dye with some deviation at lower wavelengths, while the spectral shape for picture no. 12 is quite different. Kinetic analysis of picture no. 4 yields only the intermediate rate, and the shape for picture no. 12 (at high water concentration) was obtained after several scans in order to remove any IR band that might be present. These results are in accord with earlier assignments. In Run 7.2, as shown in Figure 19, the shape deviates from that of the IR band, and shows the presence of the R band. This spectrum is similar to that obtained from picture no. 12 in Run 7.1, which is the spectrum after the intermediate reaction is finished. Since a higher cesium concentration was employed here, the appearance of the R band and the observed kinetic results (namely, the rate of 5 $M^{-1}sec^{-1}$) is not surprising.

The rapid decrease in absorbance observed at the beginning of some traces (k = 40 to 200 $M^{-1}sec^{-1}$) might be due to reaction with impurities. This would require occasional impurity concentrations in excess of 10^{-4} molar, however (cf. lithium discussion below). Further study is necessary to determine the origin of this process. Blank determinations of the rate of absorbance change upon mixing

with pure solvent indicated auto-decomposition to be much slower than the rate of reaction with the lowest concentration of water used. This too, indicates that the reaction with impurities is unimportant, although a catalytic effect could still be present.

While only one run each was made with rubidium and potassium with water in EDA, the results were quite similar to those of the cesium-water system. Although runs with the rapid-scan system would be needed before any definite conclusions can be drawn, the reaction of the IR band species with water may be tentatively assigned to the rate, $k \sim 14$ $M^{-1}sec^{-1}$. Since both rubidium and potassium solutions in EDA possess the V and R bands, as well as the IR band, no assignment can be attempted for the slower rate, $k \sim 3.5$ $M^{-1}sec^{-1}$. The presence of a fast rate in a few rubidium-water traces should also be noted.

Pulse-radiolysis studies on the disappearance of the hydrated electron through reaction with solvent gives a second-order rate constant of 16 ± 1 $M^{-1}sec^{-1}$ (10). This is in good agreement with the value 19.6 ± 4.9 $M^{-1}sec^{-1}$ obtained for the reaction of cesium with water in EDA, despite the differences between the two solvent systems. Radiation chemists have shown (77,78) that the disappearance of the hydrated electron is a reversible reaction which can be written

$$e^-_{aq} + H_2O \underset{k_2}{\overset{k_1}{\rightleftharpoons}} H + OH^-_{aq} \qquad (12)$$

If the same reactions are assumed to take place in the ethylenediamine solvent system, and if H atoms are removed by

$$H + H \xrightarrow{k_3} H_2 \qquad (13)$$

then,

$$-\frac{d[e^-]}{dt} = k_1[e^-][H_2O] - k_2[OH^-][H] \qquad (14)$$

and

$$\frac{d[H]}{dt} = k_1[e^-][H_2O] - k_2[OH^-][H] - k_3[H]^2 \qquad (15)$$

Assuming that $\frac{d[H]}{dt} = 0$, and if $[e^-] = [e^-]_o - x$ and $[OH^-] = x$, Equation 14 may be rewritten as

$$\frac{dx}{dt} = k_1[H_2O]\,([e^-]_o - x) - k_2[H]_{s.s.}\,x \qquad (16)$$

Integration of this equation gives

$$\ln \frac{k_1[H_2O][e^-]_o}{k_1[H_2O][e^-]_o - (k_1[H_2O]+k_2[H])[OH^-]} = (k_1[H_2O] + k_2[H])t \qquad (17)$$

This equation may be rearranged to yield

$$\ln[e^-] = \ln\left\{[e^-]_o - \frac{k_1[H_2O][e^-]_o}{k_1[H_2O] + k_2[H]}\,[1-\exp(k_1[H_2O]+k_2[H])t]\right\} \qquad (18)$$

Figure 20 shows a comparison of calculated values with the experimental graph of log(Abs.) *vs.* time using a rate constant of 2.2×10^7 $M^{-1}sec^{-1}$ for k_2, and $k_3 = 2 \times 10^{10}$ $M^{-1}sec^{-1}$, the values in water. A more favorable case is shown in Figure 21 for an experimental graph that shows a break. Also shown here are the calculated points using a

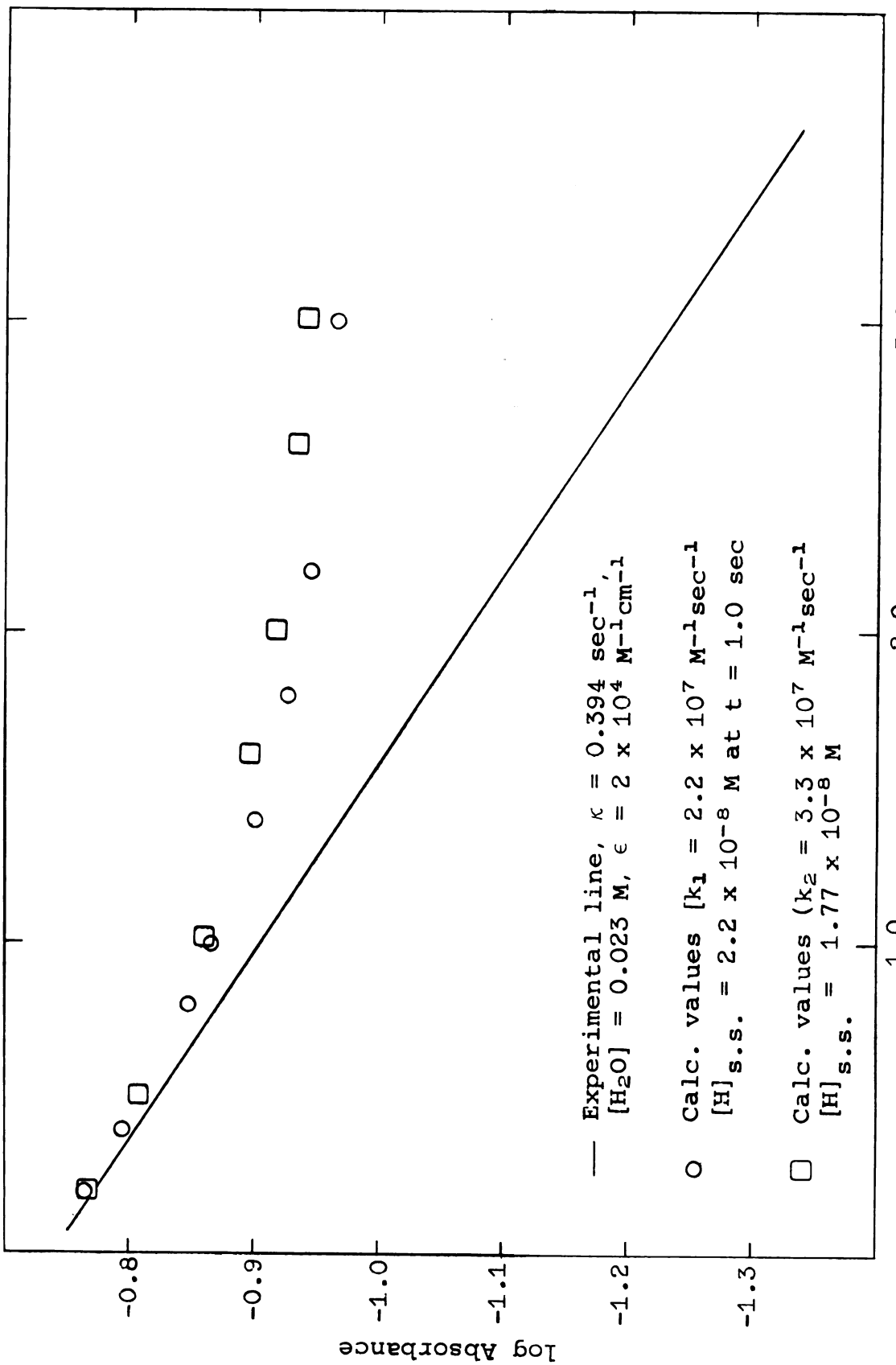

Figure 20. Comparison of an experimental graph of log (Abs.) vs. time with values calculated considering the reaction $H + OH^- \rightarrow e^- + H_2O$.

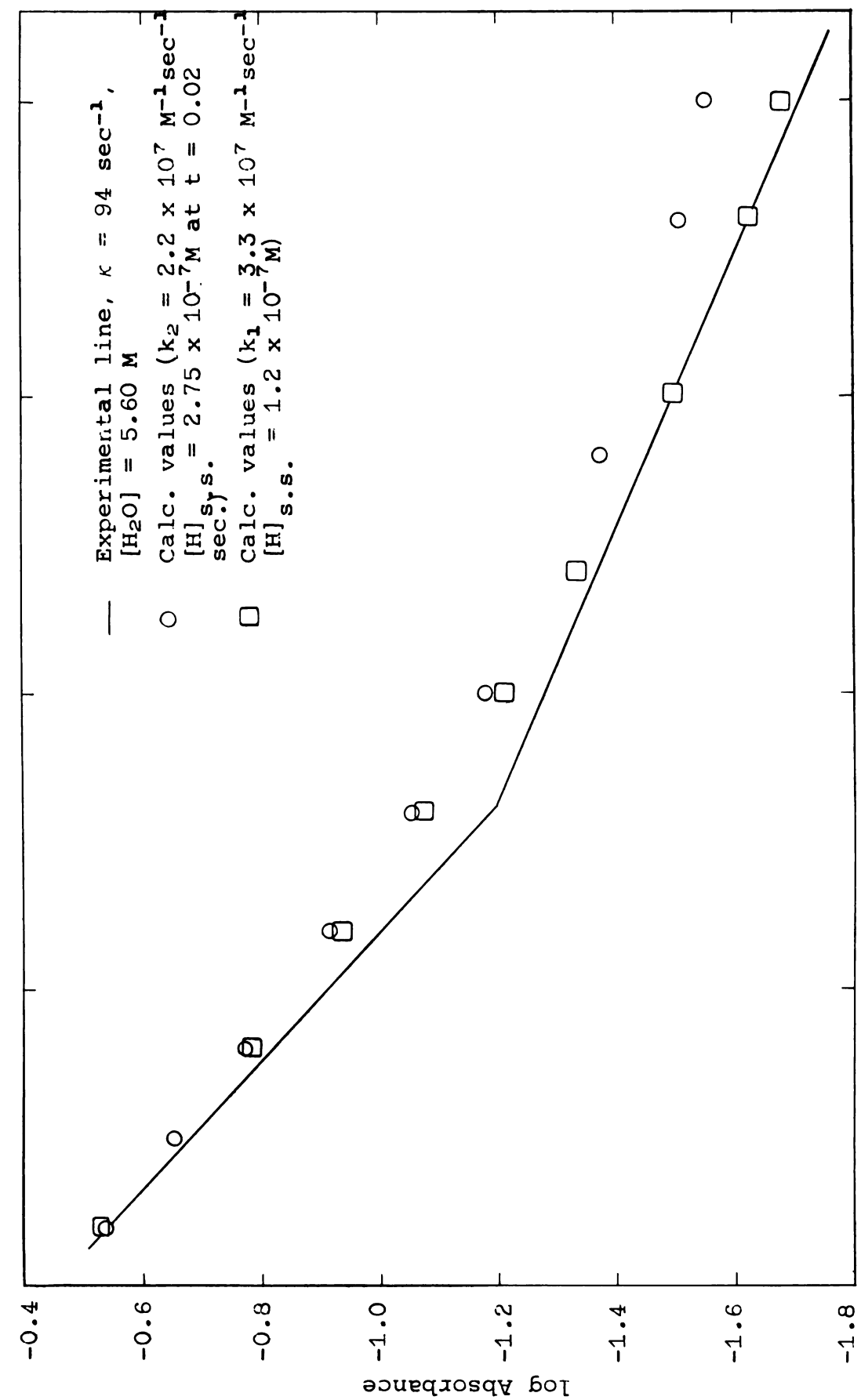

Figure 21. Comparison of an experimental graph of log (Abs.) vs. time with values calculated considering the reaction $H + OH^- \rightarrow e^- + H_2O$ for a trace showing two rates.

value of $k_2[H]_{s.s.} = 4.0$, a lower value, which decreases the importance of the back reaction in Equation 12. The fit is improved at a few points, but still differs considerably from the observed line. Surprisingly, this treatment gives the lower value of $[H]_{s.s.}$ of 1.2×10^{-7} M (as compared to the initial value of 2.76×10^{-7} M for $k_2 = 2.2 \times 10^7$ $M^{-1}sec^{-1}$), but <u>increases</u> k_2 to 3.3×10^7 $M^{-1}sec^{-1}$. Use of this latter value in Figure 20 actually worsens agreement, since $k_2[H]_{s.s.}$ goes from 4.84 to 5.84 here. An examination of Equation 17 shows that the calculated points can only agree with experiment if the reverse reaction of Equation 12 is unimportant in the water-EDA system. This is probably because hydrogen atoms are removed by another process than that of Equation 13. Such a mechanism will be discussed below in Sect. V-F. In addition, no differences were observed in the reaction of cesium with water in the presence of cesium hydroxide. This agrees with Dewald's observations upon adding KOH to the water (11), and further supports the absence of back-reaction.

When large pulse currents are used in the radiolysis of water, enough e^-_{aq} is produced so that it disappears by a bimolecular process,

$$e^-_{aq} + e^-_{aq} \longrightarrow H_2 + 2OH^-_{aq} \qquad (19)$$

with a second-order rate constant of $1.1 \times 10^{10} M^{-1}sec^{-1}$ (77). If this is written as

$$2e^-_{solv} + 2H_2O \longrightarrow H_2 + 2OH^-_{solv} \qquad (20)$$

then

$$-\frac{d[e^-]}{dt} = k\,[H_2O]^2[e^-]^2 \qquad (21)$$

and the fourth-order rate constant for this equation is $3.57 \times 10^6\ M^{-3}sec^{-1}$, in pure water. If this reaction were to take place in the water-EDA system with the same rate constant, then at a water concentration of only 0.08 M, the half-life for this reaction would be equal to that of the reaction of e^-_{EDA} with water,

$$e^-_{EDA} + H_2O \longrightarrow \tfrac{1}{2}\,H_2 + OH^- \qquad (22)$$

No evidence for such a reaction was found.

2. Sodium. The reaction of sodium with water in EDA is first-order in metal absorbance, but the order in water is not constant as shown in Figure 11. Early results (93) indicated an order of 3/2 in water, but additional runs at low water concentrations show that the apparent order is less than one at low concentrations and may be as high as two at higher water concentrations. If the V band species were dimeric as proposed by Dye and Dewald (52), then these results could be explained by considering two competitive reactions

$$M_2^+ \cdot e^- + H_2O \longrightarrow H + M_2^+ + OH^- \qquad (23)$$

and

$$M_2^+ \cdot e^- + 2H_2O \longrightarrow H_2 + 2M^+ + 2OH^- \qquad (24)$$

Reaction 23 would occur predominantly at low water concentrations and Reaction 24 at high water concentration. In considering this behavior, it must be recalled that sodium solutions show only a single absorption band with a maximum at 650 mμ (50), and exhibit conductance behavior quite different from that of the other alkali metals (51). The nature of this reaction probably will not be understood until the V band species is itself better characterized.

3. Lithium. From the four runs of lithium with water in EDA several conclusions can be drawn, but a number of questions remain to be answered. The reaction of the V band species with water must be assigned a rate of $\sim 30\ M^{-1}sec^{-1}$ on the basis of the results obtained in Run 6.2. It appears, according to Runs 2.2 and 5.3, that the fastest rate is associated with the IR band, although several traces in the latter run (cf. Table VI) do not support this view entirely, since several traces at 700 mμ also show this reaction. Since the V and IR bands do overlap significantly (50), the intermediate rate cannot be positively assigned to either band. The concentration dependence of the species present in these solutions, as well as their relative instability, make them difficult to work with. Run 7.3, carried out with the rapid-scan system, appears to yield three rate constants. The shapes of two lithium solution spectra, Figure 22, show that the solution consisted primarily of the IR band, but the presence of another species is apparent. This is

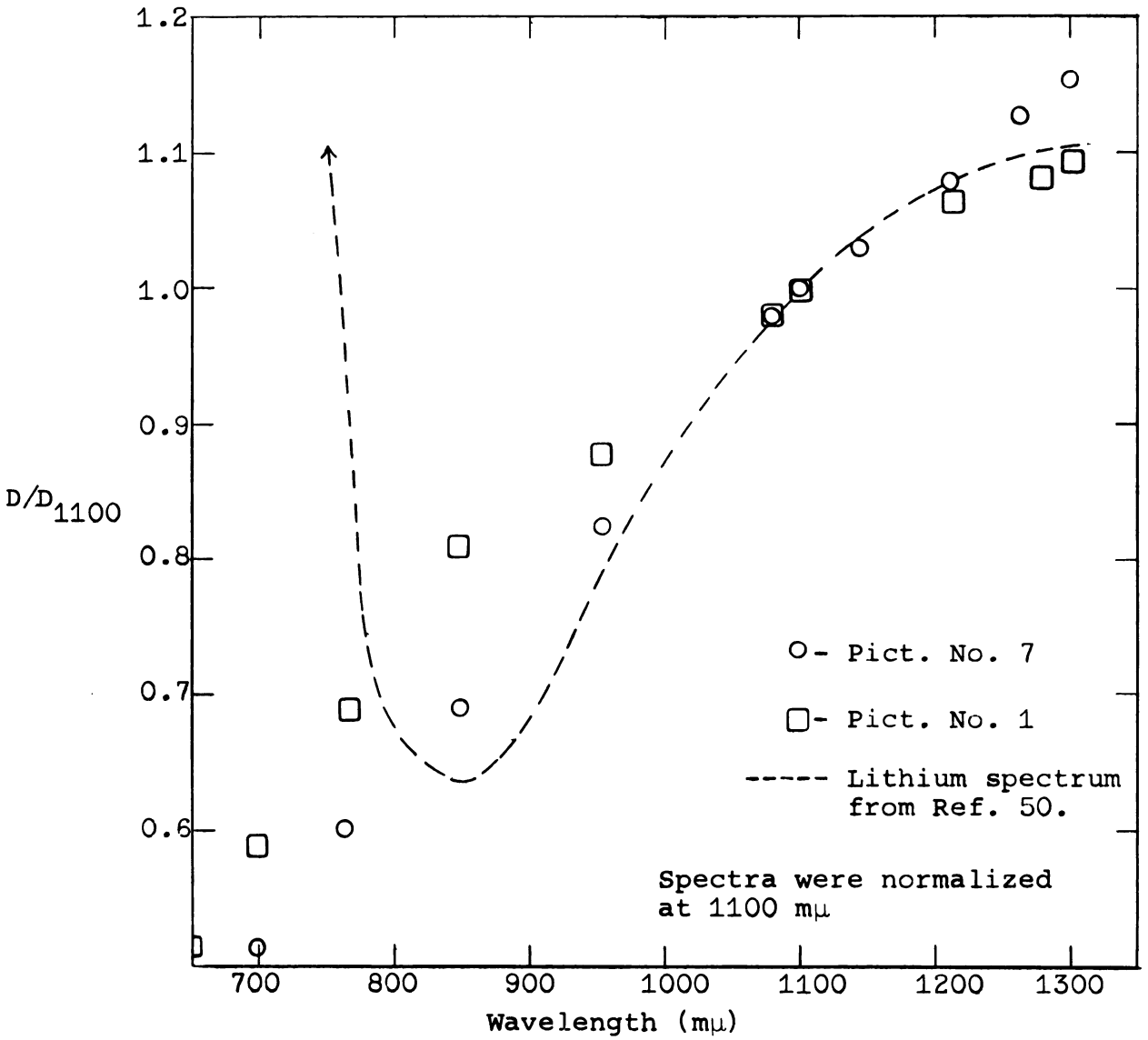

Figure 22. Comparison of the spectral shapes for typical traces of Run 7.3 with that of Dewald and Dye (50).

probably another IR species, and recalls the scheme proposed by Ottolenghi, Bar-Eli, and Linschitz (62) to explain their flash-photolysis results with alkali metal solutions in ethylamine, which requires an additional species absorbing in the IR.

Several traces from Runs 5.3 and 7.3 showing the faster rates could be fitted to second-order kinetics over about one half-life. Examples of such behavior are shown in Figure 23. However, a second-order process could be ruled out by the following argument:

If

$$-\frac{d(\text{Abs.})}{dt} = k(\text{Abs.})^2 \qquad (25)$$

then

$$\frac{1}{(\text{Abs.})} = kt + \frac{1}{(\text{Abs.})_o} \qquad (26)$$

and

$$\ln(\text{Abs.}) = -\ln\left[kt + \frac{1}{(\text{Abs.})_o}\right] \qquad (27)$$

Differentiating,

$$\frac{d\ \ln(\text{Abs.})}{dt} = -\frac{k}{[kt + 1/(\text{Abs.})_o]} \qquad (28)$$

and at $t = 0$,

$$\frac{d\ \ln(\text{Abs.})}{dt} = -k(\text{Abs.})_o \equiv -k^{app} \qquad (29)$$

A graph of this relation for Run 5.3 is given in Figure 24. This shows that the apparent rate fails to correlate with initial absorbance as required for second-order kinetics by Equation 29. It must be pointed out that by the same

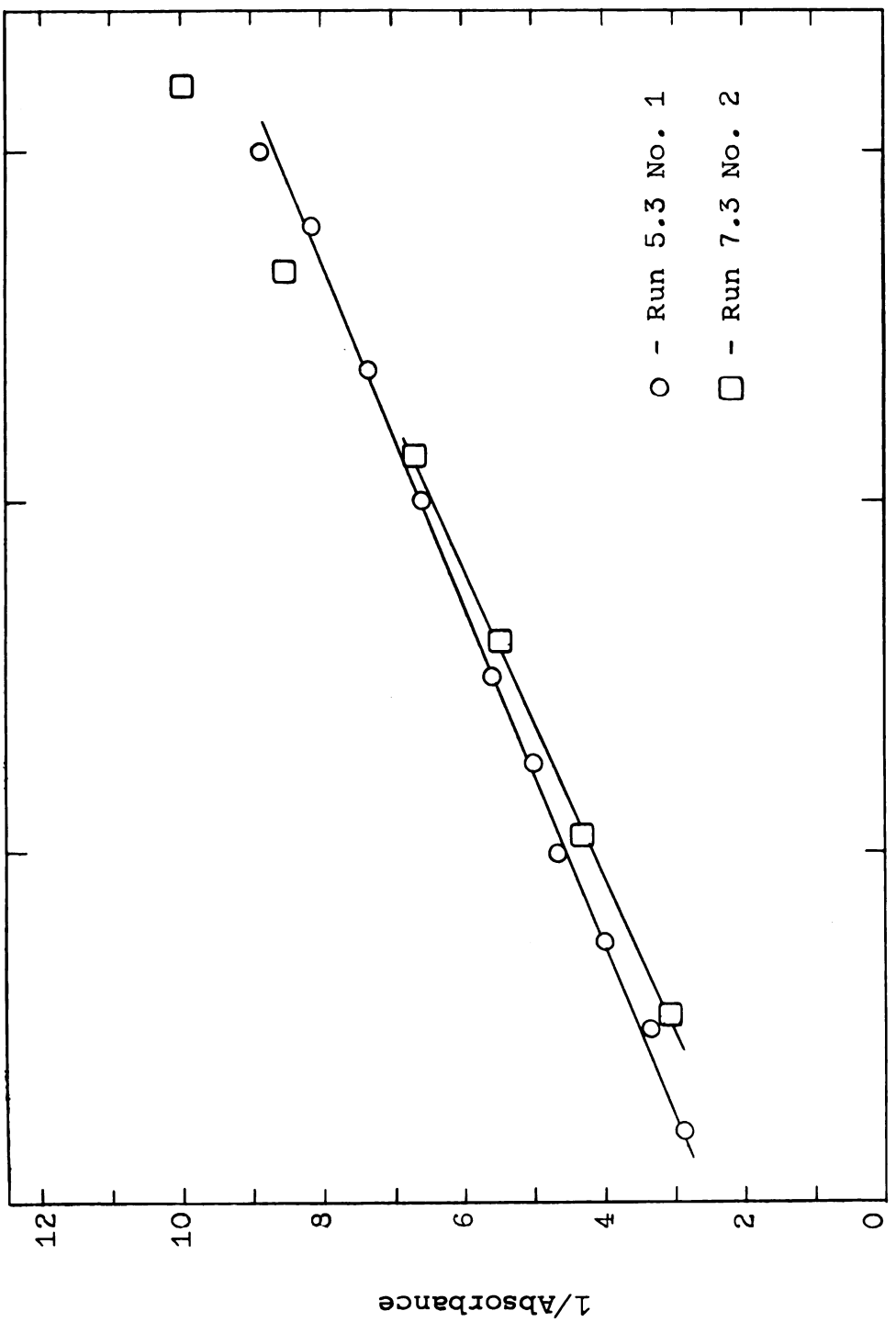

Figure 23. Plots of 1/Absorbance vs. time for the reaction of lithium with water in ethylenediamine.

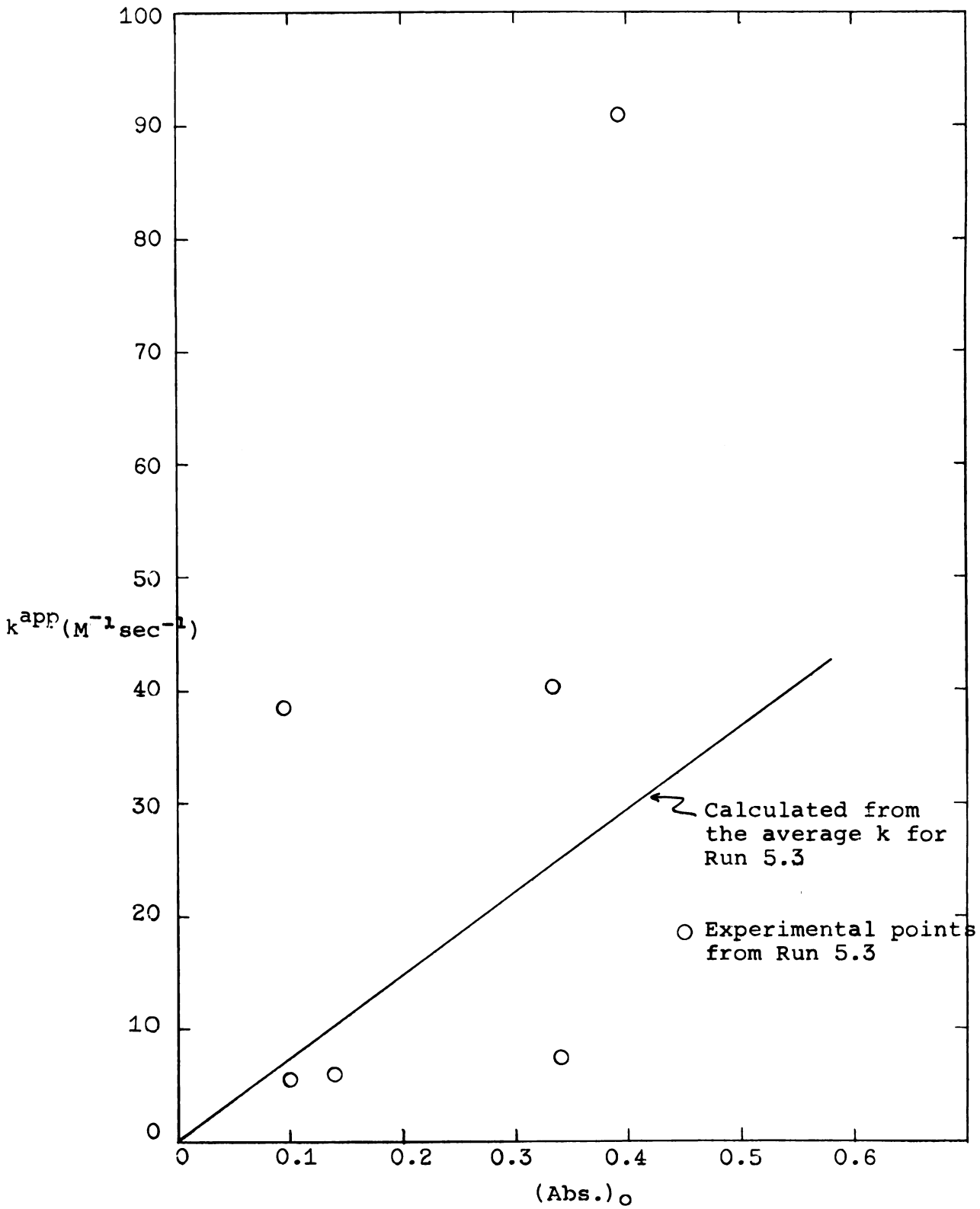

Figure 24. Graph of k^{app} vs. $(Abs.)_o$ for the reaction of lithium with water in ethylenediamine.

type of argument, the unusual amount of scatter present in the first-order rate constants (for the fast rate) could also be used to rule out this assignment.

C. Alkali Metals with Methanol and Ethanol

Although the detailed nature of the reactions with methanol and ethanol remains unknown, it is clear from these studies that the overall rate of reaction of the solvated electron with these alcohols is not far different from that with water. Pulse radiolysis studies (94) show minimum half-times of 1.5 and 3 μsec for the disappearance of the electron peak in the pure alcohols, but this does not necessarily represent reaction of the electron with the alcohol, since no attempt was made to remove the counter-ion or other radiolysis products. While Freeman (95), on the basis of competition kinetics, is inclined to accept these values as the natural lifetime of the electron in the alcohols, Anbar (9) expects that the lifetime of e^-_{solv} in alcohols will be much longer than in water. The argument of the latter author is based upon the lower stability of alkoxy ions in the alcohols which would lead to a decreased energy of solvation for the reaction

$$e^-_{solv} + ROH \longrightarrow H + OR^-_{solv} \qquad (30)$$

as R goes from H to alkyl.

D. Cesium + Ethylenediammonium and Ammonium Ions

While the reaction of the solvated electron with hydrogen ions is near the diffusion-controlled limit in aqueous and alcoholic systems (94), the reaction of hydrogen chloride in our system, which presumably gives ethylenediammonium ions, is much slower, with $k \sim 1.7 \times 10^5$ $M^{-1}sec^{-1}$. The ammonium ion, however, reacts with cesium with a rate at least an order of magnitude faster than this, indicating that appreciable proton transfer from ammonium ion to ethylenediamine does not occur. From the data of Kelly et al. (96) on the reaction of sodium with ethanol in liquid ammonia at -33.4° C, Jolly (49) has been able to estimate an upper-limit of 10^8 $M^{-1}sec^{-1}$ for the reaction of the ammoniated electron with the ammonium ion. The rate constant for the reaction of e^-_{aq} with NH_4^+, cited by Rabani (78) from radiation and photochemical studies, $\sim 1.5 \times 10^6$ $M^{-1}sec^{-1}$, is in reasonable agreement with our lower limit of 3×10^6 $M^{-1}sec^{-1}$.

E. Alkali Metals + Pure Ethylenediamine

When alkali metals in EDA were mixed with solvent alone, there occurred, in some cases, a fast increase in absorbance, followed by a slower decrease, which was then followed by the usual slow decay of absorbance with time due to reaction with the solvent or impurities. An example of this behavior is shown in Figure 25a. A similar phenomenon was also noted in several traces for the reaction of metal with water, as

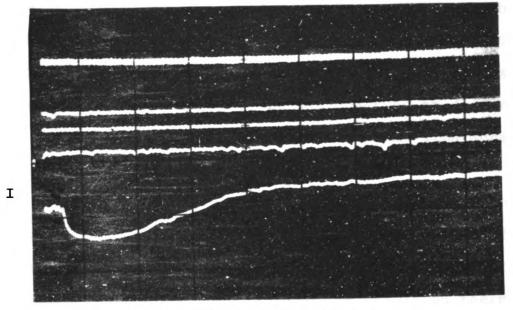

Time (0.2 sec/division)

Figure 25a. Typical trace for the reaction of cesium with pure ethylenediamine showing initial absorbance buildup.

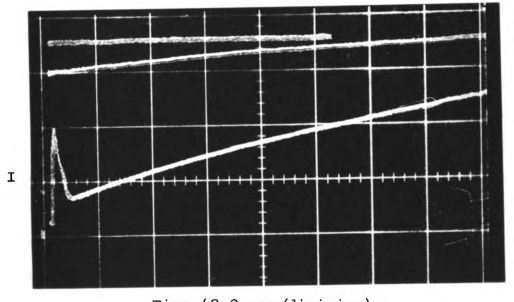

Time (2.0 sec/division)

Figure 25b. Typical trace for the reaction of sodium with water in ethylenediamine showing initial fast absorbance decrease and recovery.

shown in Figure 25b. Here, however, there was a fast decrease in absorbance, followed by a slower increase, which was then followed by the slower reaction with water. That this behavior was independent of water concentration was demonstrated in Run 5.2 where it was observed at different water concentrations, but with about the same time duration for all concentrations ($\sim$0.5 sec).

Gibson (97) has reported a change in absorbance upon mixing two portions of the same solution in a stopped-flow apparatus. This solution was at a different temperature from the mixing chamber ($\Delta t = 20^{\circ}$ C) and the resulting thermal gradients effectively made the solution act as a lens. A warm solution flowing into a cold tube gave rise to an absorbance decrease (negative lens), while a cold solution in a warm tube yielded an absorbance increase (positive lens).

The absorbance change upon mixing observed in our system is probably not an instrumental artifact of this type since: 1) it was not reproducible; 2) it occurred in cases where no heat of mixing was involved (metal-EDA with EDA), but did not occur where there was significant heat of mixing (metal-EDA with high water-EDA); 3) in all cases the mixing cell and solutions were close to 25° C; and 4) the changes were fast compared to bulk diffusion times which would be on the order of several seconds. An instrumental error of a different type could give this kind of behavior if seepage of the reactants into the mixing chamber could occur after

the flow stopped. It is puzzling, however, that the observed results did not occur with greater frequency if this were the case. If this behavior is not due to instrumental error, it is possible that upon dilution there are shifts in the equilibria among the various species, and that they give rise to the observed behavior. It is likely that impurities or decomposition products also have an influence on this process.

F. Mechanisms

Since

$$H_2O + EDA \underset{k_3}{\overset{k_2}{\rightleftharpoons}} EDAH^+ + OH^- \qquad (31)$$

with $K < 10^{-12}$ (98), it might be possible for the reaction of alkali metal (represented by e^-) with water to go through $EDAH^+$ as an intermediate. The mechanism would consist of Equation 31 and

$$e^- + EDAH^+ \longrightarrow H + EDA \qquad (32)$$

Writing $$-\frac{d[e^-]}{dt} = k_1[e^-][EDAH^+] \qquad (33)$$

and $$\frac{d[EDAH^+]}{dt} = k_2[H_2O][EDA] - k_3[EDAH^+][OH^-] - k_1[EDAH^+][e^-] \qquad (34)$$

then setting $\frac{d[EDAH^+]}{dt} = 0$, and substituting the result into Equation 33 gives

$$-\frac{d[e^-]}{dt} = \frac{k_1k_2[EDA]}{k_1[e^-] + k_3[OH^-]}[e^-][H_2O] \qquad (35)$$

or

$$-\frac{d[e^-]}{dt} = k\ [e^-]\,[H_2O] \qquad (36)$$

Since $K < 10^{-12}$, and letting k_3 have a diffusion-controlled rate of $10^{10}\ M^{-1}sec^{-1}$, then $k_2 < 10^{-2}$. For $[H_2O] > 10^{-2}$ M, $[OH^-] \sim 10^{-6}$ M by Equation 31. Then

$$k < \frac{(10^5)(10^{-2})(10)}{10^5(10^{-4}) + 10^{10}(10^{-6})} < 1 \qquad (37)$$

The value found for k in this calculation represents an upper limit. Since this is at least an order-of-magnitude less than the observed rate constant, and since no dependence of the second-order rate constant upon water concentration was observed, it seems probable that this mechanism does not compete with the direct reaction

$$e^- + H_2O \xrightarrow{k_1} H + OH^- \qquad (38)$$

It is likely that this step is followed by rapid abstraction of an alpha-hydrogen atom from EDA,

$$H + NH_2CH_2CH_2NH_2 \longrightarrow NH_2CH_2\dot{C}HNH_2 + H_2 \qquad (39)$$

analogous to the way alpha-hydrogens of ethanol react with hydrogen atoms in pulse radiolysis studies (79). The free radical produced may either react with another radical or with the reducing species. Since the overall reaction produces half a mole of hydrogen for each mole of metal reacted, the latter reaction

$$e^- + NH_2\dot{C}HCH_2NH_2 \longrightarrow NH_2CH_2CH_2NH^- \qquad (40)$$

to ultimately yield a solvent anion is more likely. A steady-state treatment of hydrogen atoms and solvent radicals gives the result

$$-\frac{d[e^-]}{dt} = 2\,k_1\,[e^-][H_2O] \qquad (41)$$

Thus with this mechanism, the observed rate constant is twice the rate constant for Reaction 38.

G. Future Work

The work of Dewald *et al.* (11,12) and the present work have effectively demonstrated the potential of this method for studying electron-attachment reactions. The present work has also pointed up the need for a better understanding of metal-amine solutions, if truly quantitative and meaningful results are to be obtained. The state of the theory of these solutions has been discussed previously (Sect. II-B), and a number of general criteria have been mentioned. In direct relation to our kinetic studies, further work is needed on the optical absorption spectra of metal solutions in EDA, particularly of stable dilute solutions. The rapid-scan system could be used in place of a slower spectrophotometer to achieve this. Certainly the nature of the V band, especially in sodium solutions, needs to be cleared up. Combined EPR and conductivity studies would be of great value here.

The use of potassium solutions for kinetic studies should be investigated, since there is a greater separation of IR and R bands in these solutions. Kinetic details of the methanol and ethanol systems, and the apparent intermediate formed need to be worked out. Studies to obtain the temperature dependence of these systems would be tedious, but might provide some useful information. Other solvents such as liquid ammonia and 1-3 propanediamine should be investigated.

Other electron-transfer reactions could be examined using the flow system. These include reactions such as

$$Cs(^{IR}_{R}) + Na^{+} \xrightarrow{EDA} Cs^{+} + Na(V) \qquad (42)$$

and inorganic reductions (99) such as

$$Zn^{+2} + e^{-} \longrightarrow Zn^{+1} \qquad (43)$$

The rate of reactions such as the latter is too high for direct measurement, but transient spectra could be studied with the rapid-scan system. Metal-amine solutions could be employed to produce organic anions which then could be used to study electron-transfer reactions. Other probable reactants for this system are those which are "unreactive" with respect to the pulsed radiolysis technique, and include both organic and inorganic compounds (100,101).

REFERENCES

1. E. J. Hart, Advances in Chemistry Series, 50, "Solvated Electron," edited by R. F. Gould, American Chemical Society, Washington, D. C., 1965, p. vii.

2. J. W. Boag and E. J. Hart, Nature, 197, 45 (1963).

3. E. J. Hart and J. W. Boag, J. Am. Chem. Soc., 84, 4090 (1962).

4. J. P. Keene, Nature, 197, 47 (1963).

5. W. Weyl, Ann. Physik, 121, 601 (1864).

6. C. A. Kraus, J. Am. Chem. Soc., 30, 1323 (1908).

7. G. Lepoutre and M. J. Sienko, editors, "Metal Ammonia Solutions; Physico-chemical Properties," W. A. Benjamin, Inc., New York, 1964.

8. L. M. Dorfman, p. 36 in Ref. 1.

9. M. Anbar, ibid., p. 55 and references therein.

10. E. J. Hart, S. Gordon, and E. M. Fielden, as quoted in Ref. 9.

11. R. R. Dewald, Ph. D. Thesis, Michigan State University, 1963.

12. R. R. Dewald, J. L. Dye, M. Eigen, and L. de Maeyer, J. Chem. Phys., 39, 2388 (1963).

13. E. J. Kirschke and W. L. Jolly, Science, 147, 45 (1965).

14. C. Kraus, J. Chem. Ed., 30, 83 (1953).

15. M. C. R. Symons, Quart. Rev., 13, 99 (1959).

16. W. L. Jolly, Progr. Inorg. Chem., 1, 235 (1959).

17. T. P. Das, Advances in Chemical Physics, 4, 303 (1962).

18. M. Ottolenghi and H. Linschitz, p. 149 in Ref. 1.

19. A. L. Cederquist, Ph. D. Thesis, Washington University, St. Louis, 1963.

20. R. C. Douthit and J. L. Dye, J. Am. Chem. Soc., 82, 4472 (1960).

21. M. Gold and W. L. Jolly, Inorg. Chem., 1, 818 (1962).

22. D. F. Burow and J. J. Lagowski, p. 125 in Ref. 1.

23. C. W. Orgeel, A. M. Filbert, and E. C. Evers, p. 67 in Ref. 7.

24. S. Gunn, ibid., p. 76.

25. W. H. Brendly, Jr., and E. C. Evers, p. 111 in Ref. 1.

26. J. L. Dye, R. F. Sankuer, and G. E. Smith, J. Am. Chem. Soc., 82, 4797 (1960).

27. J. C. Thompson, p. 96 in Ref. 1.

28. C. A. Kraus and E. C. Evers, p. 1. in Ref. 1.

29. E. Huster, Ann. Physik, 33, 477 (1938).

30. S. Freed and N. Sugarman, J. Chem. Phys., 11, 354 (1943).

31. C. A. Hutchison, Jr., and R. C. Pastor, ibid., 21, 1959 (1953).

32. D. E. O'Reilly, ibid., 41, 3729 (1964).

33. T. R. Hughes, ibid., 38, 202 (1963).

34. R. A. Ogg, Phys. Rev., 69, 668 (1946).

35. W. N. Lipscomb, J. Chem. Phys., 21, 52 (1953).

36. H. A. Stairs, ibid., 27, 1431 (1957).

37. J. Jortner, S. A. Rice, and E. G. Wilson, p. 222 in Ref. 7.

38. J. Jortner, J. Chem. Phys., 30, 839 (1959).

39. A. S. Davydov, J. Expt. Theoret. Phys. U.S.S.R., 18, 913 (1948).

40. M. F. Deigen, Trudy Inst. Fiz., Akad. Nauk Ukr. S.S.R., 5, 119 (1954).

41. E. Becker, R. H. Lindquist, and B. J. Alder, J. Chem. Phys., 25, 971 (1956).

42. J. L. Dye, G. E. Smith, and R. F. Sankuer, J. Am. Chem. Soc., 82, 4803 (1960).

43. M. Gold, W. L. Jolly, and K. S. Pitzer, J. Am. Chem. Soc., 84, 2264 (1962).

44. D. E. O'Reilly, J. Chem. Phys., 41, 3736 (1964).

45. J. L. Dye and L. H. Feldman, unpublished results.

46. E. Arnold and A. Patterson, Jr., p. 285 in Ref. 7.

47. E. Arnold and A. Patterson, Jr., J. Chem. Phys., 41, 3089 (1964).

48. S. Golden, C. Guttman, and T. R. Tuttle, Jr., J. Am. Chem. Soc., 87, 135 (1965).

49. W. L. Jolly, p. 27 in Ref. 1.

50. R. R. Dewald and J. L. Dye, J. Phys. Chem., 68, 121 (1964).

51. R. R. Dewald and J. L. Dye, ibid., 128.

52. J. L. Dye and R. R. Dewald, ibid., 135.

53. K. D. Vos and J. L. Dye, J. Chem. Phys., 38, 2033 (1963).

54. K. Bar-Eli and T. R. Tuttle, Jr., Bull. Am. Phys. Soc., 8, 352 (1963).

55. K. Bar-Eli and T. R. Tuttle, Jr., J. Chem. Phys., 40, 2508 (1964).

56. T. R. Tuttle, Jr., and K. Bar-Eli, Abstracts, 146 th National Meeting of the American Chemical Society (January 1964), p. 7D.

57. L. R. Dalton, J. D. Rynbrandt, E. M. Hansen, and J. L. Dye, submitted to J. Chem. Phys.

58. D. E. O'Reilly and T. Tsang, J. Chem. Phys., 42, 3333 (1965).

59. M. Ottolenghi, K. Bar-Eli, H. Linschitz, and T. R. Tuttle, Jr., ibid., 40, 3729 (1964).

60. J. L. Dye, L. R. Dalton, and E. M. Hansen, Abstracts, 149 th National Meeting of the American Chemical Society (April 1965), p. 45S.

61. J. L. Dye, personal communication.

62. M. Ottolenghi, K. Bar-Eli, and H. Linschitz, J. Chem. Phys., 43, 206 (1965).

63. A. Ulland and J. L. Dye, unpublished results.

64. M. Anbar and E. J. Hart, J. Phys. Chem., 69, 1244 (1965).

65. A. Debierne, Ann. Physique (Paris), 2, 97 (1914).

66. N. F. Barr and A. O. Allen, J. Phys. Chem., 63, 928 (1959).

67. J. T. Allan and G. Scholes, Nature, 187, 218 (1960).

68. E. Hayon and J. Weiss, J. Chem. Soc., 5091 (1960).

69. P. J. Dyne, D. R. Smith, and J. A. Stone, Ann. Rev. of Phys. Chem., 14, 313 (1963).

70. G. Czapski, J. Jortner, and G. Stein, J. Phys. Chem., 65, 964 (1961).

71. J. W. T. Spinks and R. J. Woods, "An Introduction to Radiation Chemistry," John Wiley & Sons, New York, 1964, Chap. 8.

72. G. Czapski and H. A. Schwartz, J. Phys. Chem., 66, 471 (1962).

73. M. S. Matheson, P. 45 in Ref. 1.

74. R. L. Platzman, "Basic Mechanisms in Radiobiology," U. S. Nat. Acad. Sci. Pub. No. 305, 1953, p. 34.

75. T. J. Sworski, p. 263 in Ref. 1.

76. P. N. Moorthy and J. J. Weiss, ibid., p. 180.

77. M. S. Matheson and J. Rabani, J. Phys. Chem., 69, 1324 (1965).

78. J. Rabani, p. 242 in Ref. 1.

79. L. M. Dorfman and I. A. Taub, J. Am. Chem. Soc., 85, 2370 (1963).

80. M. C. Sauer, Jr., S. Arai, and L. M. Dorfman, J. Chem. Phys., 42, 708 (1965).

81. J. J. J. Myron and G. R. Freeman, Can. J. Chem., 43, 381 (1965).

82. R. W. Ahrens, B. Suryanarayana, and J. E. Willard, J. Phys. Chem., 68, 2947 (1964).

83. D. M. J. Compton, J. F. Bryant, R. A. Cesena, and B. L. Gehman, submitted to Rad. Res.

84. B. Chance, J. Franklin Inst., 229, 455, 613, 737 (1940).

85. Q. H. Gibson, J. Physiol., 117, 49P (1952).

86. F. J. W. Roughton and B. Chance, Technique of Organic Chemistry, VIII, edited by S. L. Friess, E. S. Lewis, and A. Weissberger, Interscience Publishers, New York, 1963, p. 703.

87. E. F. Caldin, "Fast Reactions in Solution," John Wiley & Sons, Inc., New York, 1964, Chap. 3.

88. B. Chance, et al., editors, "Rapid Mixing and Sampling Techniques in Biochemistry," Academic Press, Inc., New York, 1964.

89. (a) Electronic Scanning Spectrometer, ITT Industrial Laboratories, Fort Wayne, Indiana.
(b) Rapid Scan Monochromator, Perkin-Elmer Corp., Norwalk, Connecticut.
(c) Millisecond Wavelength Scanning Spectrometer, Control Instrument Division, Warner & Swasey Co., Flushing, New York.

90. W. Niesel, D. W. Lübbers, D. Schneewolf, J. Richter, and W. Botticher, Rev. Sci. Instr., 35, 578 (1964).

91. K. D. Vos, Ph. D. Thesis, Michigan State University, 1962.

92. G. Dulz and N. Sutin, Inorg. Chem., 2, 917 (1963).

93. L. H. Feldman, R. R. Dewald, and J. L. Dye, p. 163 in Ref. 1.

94. I. A. Taub, D. A. Harter, M. C. Sauer, Jr., and L. M. Dorfman, J. Chem. Phys., 41, 979 (1964).

95. G. R. Freeman, personal communication to J. L. Dye.

96. E. J. Kelly, H. V. Secor, C. W. Keenan, and J. F. Eastham, J. Am. Chem. Soc., 84, 3611 (1962).

97. Q. H. Gibson, p. 115 in Ref. 88.

98. M. Stafford, M.S. Thesis, Michigan State University, 1963; and J. L. Dye, personal communication.

99. G. E. Adams, J. H. Baxendale, and J. W. Boag, Proc. Chem. Soc., 241 (1963).

100. E. J. Hart, S. Gordon, and J. K. Thomas, J. Phys. Chem., 68, 1271 (1964).

101. J. K. Thomas, S. Gordon, and E. J. Hart, ibid., 1524 (1964).

102. E. J. Hart, E. M. Fielden, L. R. Dalton, and J. L. Dye, personal communication.